UCRL-LR-107476 Vol 1
Distribution Category UC-802

Preliminary Near-Field Environment Report Volume I: Technical Bases for EBS Design

Dale G. Wilder

Manuscript date: April 1993

LAWRENCE LIVERMORE NATIONAL LABORATORY
University of California • Livermore, California • 94551

Contents

Acronyms and Abbreviations

ACD	advanced conceptual design
APD	areal power density
BP	boiling point
CHnv	Calico Hills, nonwelded, vitric
CHnz	Calico Hills, nonwelded, zeolitized
DOE	U.S. Department of Energy
EBS	engineered barrier system
ECM	equivalent continuum model
ESF	Exploratory Studies Facility
GTUF	G-Tunnel Underground Facility
HLW	high-level waste
LA	license application
LAD	license application design
LLNL	Lawrence Livermore National Laboratory
NF	near field
NFE	near-field environment
NFER	*Near-Field Environment Report*
NTS	Nevada Test Site
PPw	Prow Pass, welded
PTn	Paintbrush, nonwelded
PWR	pressurized water reactor
QA	quality assurance
RIB	*Reference Information Base* (DOE, 1990)
RMR	rock-mass rating
SCP	*Site Characterization Plan* (DOE, 1988)
TCw	Tiva Canyon, welded
Tpt	Topopah Spring Member of the Paintbrush tuff
TSw1	Topopah Spring, welded, lithophysae-rich
TSw2	Topopah Spring, welded, lithophysae-poor
TSw3	Topopah Spring, welded, vitric
UNE	underground nuclear explosion
WP	waste package
WPP	*Waste Package Plan* (Harrison-Giesler, 1991)
XRD	x-ray diffraction
YM	Yucca Mountain
YMP	Yucca Mountain Site Characterization Project
YMPO	Yucca Mountain Site Characterization Project Office

1.0 Introduction

The United States Department of Energy (DOE) is investigating the suitability of Yucca Mountain as a potential site for the nation's first high-level nuclear waste repository. The site is located about 120 km northwest of Las Vegas, Nevada, in an area of uninhabited desert (Fig. 1). Lawrence Livermore National Laboratory (LLNL) is a Yucca Mountain Site Characterization Project (YMP) participant and is responsible for the development of waste package (WP) and engineered barrier system (EBS) design concepts, including materials testing and selection, design criteria development, waste-form characterization, performance assessments, and near-field environment (NFE) characterization. Materials testing, design criteria and concept development, and waste-form characterization all require an understanding of the environmental conditions that will interact with the WP/EBS. The *Preliminary Near-Field Environment Report* (NFER) has been identified in the *Waste Package Plan* (WPP) (Harrison-Giesler, 1991) as the formal means for transmitting and documenting this information. Glassley (1986) summarized the expected near-field environmental conditions as understood at that time. The purpose of this report is to provide an update of that report, reflecting the current understanding of the environmental conditions. Because the design and performance of the WP and the EBS will be dependent on the geomechanical, hydrologic, and geochemical conditions over time in the rock forming the NFE, greater emphasis is placed in this report on the processes that change the environmental conditions and what will likely be the changed conditions.

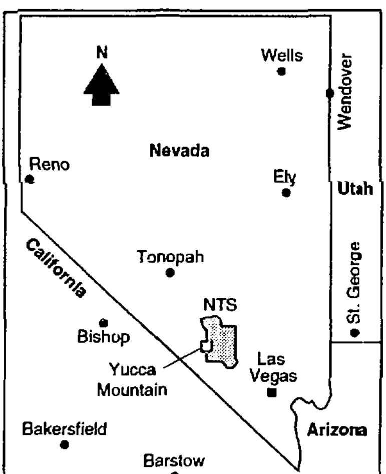

Figure 1. The Yucca Mountain site is located about 120 km northwest of Las Vegas, Nevada.

Favorable aspects of Yucca Mountain as a potential repository site relate to its arid nature and the sorptive properties of the rock materials. The arid environment results in unsaturated conditions at the potential emplacement horizon. The major advantages of unsaturated conditions are that container corrosion, waste-form leaching, and radionuclide transport mechanisms are minimized because of the lack of contact between liquid water and the WP. The Topopah Spring Member of the Paintbrush tuff (Tpt) at Yucca Mountain, which is anticipated to be unsaturated, was selected for suitability studies as a potential repository horizon. Although the *Reference Waste Package Environment Report* (Glassley, 1986) and the *Site Characterization Plan* (SCP) (DOE, 1988) describe the NFE of the potential repository site, the information provided has since progressed considerably; this report provides the information developed subsequent to those earlier reports.

Volume I provides the technical bases for design of the EBS based on our current knowledge of the NFE. Volume II, *Scientific Overview of Near-Field Environment and Phenomena,* consists of eight individual reports (Secs. 1.0–8.0) that give a more detailed discussion of the topics in Vol. I as they pertain to a particular field of study. The last report in Vol. II (Sec. 9.0) is a summary of the results of field tests performed in G-Tunnel at the Nevada Test Site (NTS) near Yucca Mountain.

Much of what is known about the NFE is limited by lack of access to the emplacement horizon and by limited sample availability. In many cases, the technology for assessing the environment is under development. In addition, the NFE depends on many processes and design details that are not determined at this time. Quantitative analyses of the actual NFE must incorporate into models the information from EBS and repository design, operational practices and sequences, and performance assessments. Most of this information is either not available at this time or is only available in a preliminary form. Evaluations of the expected NFE are based on the current understanding of properties, parameters, analyses, and assumptions, as well as reference designs, and on prototype or scoping tests and analyses. In some cases, information from similar rock types or formations as well as from specific mineral or chemical conditions is used.

For the above reasons, this report will focus not only on providing parameter values but also on the processes that influence those parameters and on the impacts of those parameters on the performance of EBS components. The description of the NFE in this report should be viewed as preliminary and may not accurately represent specific conditions that will be found at Yucca Mountain once underground access is achieved. Future assessments will be required to determine whether the environment as described here is appropriate for conditions at Yucca Mountain (see Sec. 1.2 for a discussion of report updates).

1.1 NFE and the Design and Performance of the EBS

The EBS will function in an environment that will influence its performance. To develop the strategy for and to properly design the components of the EBS, information is needed on the environmental conditions expected over the lifetime of the repository. The conditions that may significantly impact the performance of the EBS and the WP and their ability to contribute to the isolation of radioactive waste are of particular interest. However, a description of the environment from a detailed scientific basis is not sufficient for design criteria and decisions; a higher-level roll-up is needed. For example, the degree of rock saturation is a very important aspect of the environment, and many of the WP designs and configurations are based on unsaturated rock conditions. However, this by itself does not provide the information needed for design. The amount, timing, and temporal distribution (steady state or episodic) of water contacting waste is what is pertinent to the design, not what the rock saturation happens to be. To estimate the amount of water expected to contact waste, we must integrate the saturation data with other factors, including (1) fracture-matrix flow models, (2) fracture distribution, (3) emplacement configuration, (4) projected WP thermal characteristics, (5) repository design, and (6) areal power density (APD). Detailed technical information is critical to performance analyses, but the focus of this volume is on the integration of values.

1.1.1 WP/NFE Interactions

Major interactions between the NFE and the EBS components involve the mechanical loading imposed on container materials and waste forms by the host rock environment; the amount of fluids and vapor or gases that contact the container or waste forms; the chemical composition of those fluids and vapors, and the retardation and sorption or exchange of radionuclides with NFE minerals and fluids; and thermal interactions between the EBS and the environment. All of these interactions are strongly influenced by the elevated temperatures that result from waste emplacement. Interaction between the EBS components and the NFE is to a large extent dominated by the possible presence of liquid water. For example, corrosion mechanisms of most candidate container materials are almost exclusively aqueous; leaching of most of the radionuclides from the waste forms is also almost exclusively dependent on the presence of liquid water; and transport of nuclides through the rock mass is exclusively dependent on aqueous mechanisms except for gaseous radionuclides associated with spent fuel (gaseous nuclides have been removed from the glass waste form and the only potential ones of concern are those generated slowly by radioactive decay).

Thus, an assessment of the major environmental impacts on EBS performance can focus on the hydrologic aspects (particularly the liquid phase) and associated geochemistry. Under matrix-dominated flow conditions, water transport will be minimal to nonexistent because capillarity will prevent moisture movement from the matrix into openings unless saturation builds up around the opening. Thus, if radionuclide transport does occur, it will most likely involve fracture flow. Because both aqueous and gaseous release pathways will very likely be dominated by the fracture network system rather than the matrix pore interconnections, the fracture system as best understood is discussed in this report.

The environmental basis for design will change with time in that the preconstruction/preemplacement conditions will be heavily influenced or changed by waste emplacement and processes associated with waste emplacement, and they will be further influenced by processes associated with repository closure. Environmental data regarding the preconstruction conditions are largely available within the *Yucca Mountain Project Reference Information Base* (RIB) (DOE, 1990) and published reports on site characterization results. Information on the postemplacement and postclosure environments also must be based on model predictions and laboratory tests at elevated temperatures. Because the radiation and thermal loading decay with time, the environment will not be static, and because of natural heterogeneities as well as nonuniform engineering or operation considerations, the environment will have spatial variability. Therefore, the information relative to postemplacement time periods will not consist of single or constant values, but rather functional relationships, graphs, etc. The reader should be aware of these differences since the lack of directly observable data can make the uncertainties far greater for the postemplacement and postclosure periods.

Because the environmental conditions are expected to change in response to construction and emplacement, some of the processes that may impact the environment are discussed. It is not intended that this be an all inclusive list, but rather that the discussion alert the reader to the potential impact that various design decisions may have on the environment.

1.1.2 NFE vs Overall Repository Environment

The term "near field" is used to distinguish the environmental conditions impacting WPs from those existing beyond the zone having direct influence on the WP. The NFE is defined more on the basis of impacts on the WP design and performance than on geometric scale. The impact can extend to considerable distances for some processes (e.g., the change in water conditions that may extend much beyond 50 m from the emplacement opening), and for other processes (e.g., radiolysis), the impact may be limited to very small distances from the borehole or emplacement drift.

It is important to recognize that although overall repository properties are important to consider in making an assessment of the WP or EBS system, processes and events that are expected to occur as a result of construction activities and waste emplacement may modify or perturb existing environmental conditions in the near field. Consequently, the WP or EBS system may not be in an environment that is the same as the overall repository. The environment of the near field, which will have an impact on the WP and its performance, may appropriately be called the environment of the altered zone .

1.1.3 Reference Design

The engineering design of the EBS and repository, as well as operational considerations (e.g., sequence of emplacement, ventilation rates, age and mix of waste), can have a significant effect on the EBS's interaction with the environment and thus the performance of the overall system. Because the design has not been finalized, it is important to have a conceptual design in order to evaluate the environment. At the time of this report and for several years preceding this report, the reference design was as described in the SCP. The reference design concept uses emplacement in vertical boreholes, with 57 kW/acre APD. It was assumed that the waste would consist of either spent fuel approximately 10-yr out of core or glass high-level-waste (HLW) form. The studies discussed in this report focus on the spent fuel since temperatures are a factor in many of the environmental issues. Some calculations were performed for a horizontal emplacement design in order to compare approaches and results from other projects and participants. It should also be noted that some discussion will address drift emplacement rather than the use of boreholes. However, unless specified, the reference design configurations are those addressed in this report.

1.2 Relation to the *Waste Package Plan*, Other Documents, and Users

The NFER is identified in the WPP as a document that will provide information to support activities in development of design concepts. In addition, the NFER will provide information to support activities such as performance assessment, material selection, and waste form characterization. The NFER either will be updated as information becomes available, or a subsequent version will be issued which will supersede this report. Four scheduled revisions are identified in the WPP. The first will be a revision to incorporate more complete information on the technical bases for EBS design (Vol. I). This revision will be made approximately one year after first issuance of the NFER. An updated NFER will be produced after surface-based cores are available for testing. It is planned that this report will be produced during the early stages of the advanced conceptual design (ACD) phase so that information will be available for the ACD. A revision of the updated NFER will be issued on the basis of the availability of large block samples from the Exploratory Studies Facility (ESF) construction. The revised updated NFER is intended to support the license application design (LAD) phase. Another revision of the NFER will be issued once the ESF testing results are available, and that report will be the one used in support of the license application (LA). No further reports are discussed in the WPP, although it is recognized that there will likely be reports that cover subsequent work related to performance confirmation phase work.

1.3 Quality Assurance (QA) Controls

The *Preliminary Near-Field Environment Report* is a non-quality-affecting report because of its intended use: to provide preliminary information on the NFE for use in conceptual design and in formulating strategy/option definitions. Much of the data in this first version of the NFER are either (1) not based on parameter measurements of materials representative of the actual potential repository horizon, or (2) based on measurements made on samples or core with undeterminable QA pedigrees. The data are intended to provide scientific understanding and information that will be useful for future activities, such as measurements and analyses, rather than to provide values to be used for licensing directly. Subsequent revisions or companion reports in which the data reported are based on testing of actual materials from the potential repository horizon will serve as the basis for LA information; the appropriate QA controls will be determined for these subsequent documents.

2.0 Preemplacement NFE

Yucca Mountain consists of a series of variably fractured, nonwelded to densely welded tuff units with an eastward tilt of about 5 to 30° (Montazer and Wilson, 1984). The thickness of the unsaturated zone varies from 500 to 750 m. The potential repository is located within this unsaturated zone, lying approximately 350 m below the ground surface and 225 m above the water table (Klavetter and Peters, 1988). Montazer and Wilson (1984) also report the absence of perennial streams at Yucca Mountain. Therefore, recharge due to rainfall occurs episodically. Flint (1991) reports that the mean annual precipitation at Yucca Mountain varies (areally) from 150 to 240 mm/yr. Overall infiltration is expected to be very low. Flux estimates based on equivalent continuum model (ECM) analysis for the repository horizon range from 0.05 to 1.0 mm/yr, with a possibly upward direction due to vapor transport from the underlying saturated zone (see Vol. II, Sec. 1.0) (Montazer and Wilson, 1984).

The geologic unit being considered as the host rock is in the Topopah Spring Member of the Paintbrush tuff (Tpt). The welding within the Topopah Spring tuff (Tpt) results in a highly fractured rock mass. Estimates of fracture density (based on core) range from 20 to 42 fractures m^3 (MacIntyre et al., 1990; Scott and Castellanos, 1984; Dudley et al., 1990; Wilder, 1990). Fracture aperture estimates range from 43 to 127 μm (Buscheck, 1990). As is discussed in greater detail in Vol. II, this fracturing has a major impact on the NFE. The Tpt is a formal stratigraphic unit and has been subdivided into more specific thermal/mechanical units, which are particularly useful for hydrologic analyses. Both the formal and thermal/mechanical stratigraphic columns are shown in Fig. 2 (Nimick and Schwartz, 1987). The potential repository horizon is in the thermal/mechanical TSw2 unit (Ortiz et al., 1985), which is a devitrified, welded, rhyolitic tuff that is moderately to densely welded tuff, and appears to consist of a mass of intact blocks separated by ubiquitous planar cooling fractures that tend to be strata bound and by discrete tectonic fractures that may not be planar but tend to be more extensive. Price et al. (1987) report that the majority of the rock is a fine-grained matrix and contains gray-colored regions of vapor-phase-altered material that vary in size and are quite common. In addition to these main components, the rock contains small (open and closed) lithophysal and "healed" fractures filled with quartz or calcite.

2.1 Geochemistry

Petrographic analysis shows that the repository horizon tuff consists of (1) primary minerals, such as sanidine, plagioclase, quartz, biotite, iron-titanium oxides, allanite and zircon, which formed at temperatures in excess of 600°C in a magma chamber prior to eruption of the tuff, and (2) secondary minerals, such as cristobalite, quartz, alkali feldspars, and smectite clays, which formed during cooling and later alteration of the tuff at temperatures less than 500°C. The chemical composition of the rock is shown in Table 1. Because these values were determined from cores, they may not be representative of the composition of mineral coatings along fractures.

Distinguished from the primary and secondary minerals are the minerals that formed on fracture surfaces [e.g., calcite, smectite, quartz, cristobalite, alkali feldspar, and the zeolites mordenite, chabazite, clinoptilolite, and heulandite (Carlos, 1985, 1989; Lin and Daily, 1989)]. These minerals form layers that possess physical properties distinct from those minerals in the rock matrix and are estimated to be a maximum of 5% of the total rock mass. The mineral assemblage along a fracture surface varies from one location to another and appears to reflect, at least in part, the previous location of the saturated zone (Carlos, 1989). On the basis of x-ray diffraction (XRD) analyses, the mineral assemblage of a typical fracture surface within the repository horizon might consist of 7% smectite, 7% cristobalite, 12% quartz, 29% clinoptilolite, and 45% alkali feldspar (Carlos, 1985).

See Glassley (1986) for a more detailed discussion and description of the mineralogic and chemical properties of the preemplacement environment.

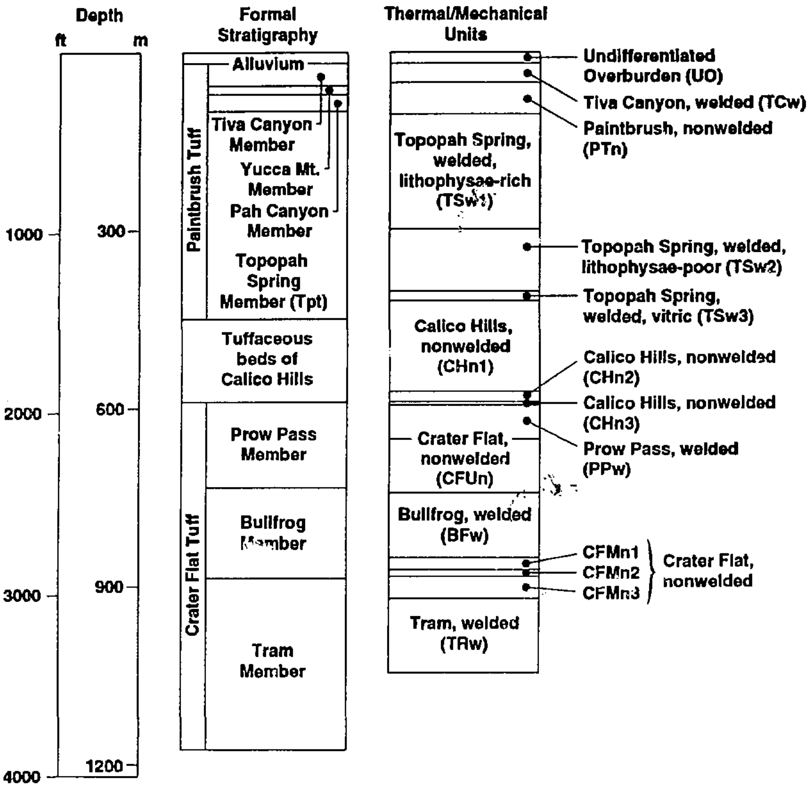

Figure 2. Relationship of formal stratigraphy and thermal/mechanical units. Adapted from Nimick and Schwartz (1987).

2.2 Hydrology

Because of the small pore size and the unsaturated conditions, a significant suction potential (matrix potential, capillary force or suction) develops in the rock. LLNL performed suction potential tests at room temperature and at elevated temperatures. Tests at room temperature were performed to be consistent with tests of others. It is recognized that these tests may not be representative of conditions at Yucca Mountain after waste is emplaced, or even of ambient conditions considering existing geothermal gradients. Suction potential results from LLNL tests are shown in Figs. 3 and 4. Considerable variability is shown among these samples, implying a heterogeneity of suction properties in the Topopah Spring tuff. LLNL data show approximately a factor of 3 difference in suction potential between samples 1 and 3 at 15% saturation. Nevertheless, the room temperature drying data of our measurements are within the spread of corresponding psychrometer results of

Table 1. Percentages of major constituents in Topopah Spring tuff (core samples 60, 61, and 62 from drill hole USW G-3). Fe_2O_3 represents total iron. Data from Schuraytz et al. (1986).

Constituent	60	61	62	Average	Std dev
SiO_2	78.4	78.9	78.9	78.73	0.24
Al_2O_3	12.0	12.3	12.2	12.17	0.12
Fe_2O_3	1.016	0.973	1.000	0.996	0.018
CaO	0.492	0.451	0.480	0.474	0.017
MgO	0.1271	0.1281	0.1126	0.123	0.007
TiO_2	0.1108	0.0927	0.0984	0.101	0.008
Na_2O	4.07	3.92	4.25	4.08	0.13
K_2O	3.71	3.18	2.94	3.28	0.32
P_2O_5	0.01	0.01	0.03	0.02	0.01
MnO	0.0624	0.0455	0.0488	0.052	0.007

Klavetter and Peters (1987). At 20°C, there is a measurable hysteresis between drying and wetting data.

The saturated water permeability of an intact Topopah Spring tuff sample at room temperature measured by LLNL is about 0.3 μD, although measurements by others (Moore et al., 1986) at room temperature ranged from 0.85 to 64 μD. The saturated water permeability of fractured Topopah Spring tuff is at least three orders of magnitude greater than that of intact tuff. At room temperature, cylindrical tuff samples containing a single natural hair-line through-fracture have apparent water permeabilities ranging from 0.85 to 13 mD (Daily et al., 1987). The water permeability of an intact Topopah Spring tuff sample is virtually independent of temperature, time, and the dehydration and rehydration processes.

The matrix properties of the hydrostratigraphic units at Yucca Mountain are summarized in Table 2 (Klavetter and Peters, 1988). The units generally fall into two categories: (1) welded tuffs of very

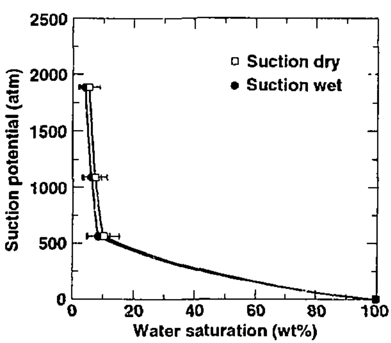

Figure 3. Suction potential as a function of water saturation at 20°C for Topopah Spring tuff.

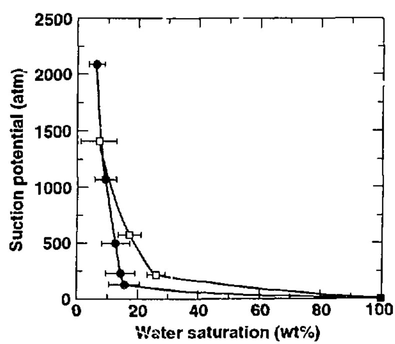

Figure 4. Suction potential as a function of water saturation at 70°C for Topopah Spring tuff.

Table 2. Matrix properties of Yucca Mountain tuff (Klavetter and Peters, 1988).

Unit[a]	Sample code	Porosity	Permeability (m^2)	S_r[b]	α[c] $10^{-2}\ m^{-1}$	β[c]
TCw	G4-1	0.08	9.7×10^{-19}	0.002	0.821	1.558
PTn	GU3-7	0.40	3.9×10^{-14}	0.100	1.500	6.872
TSw1	G4-6	0.11	1.9×10^{-18}	0.080	[illegible]	1.798
TSw2	G4-6	0.11	1.9×10^{-18}	0.080	0.567	1.798
TSw3	GU3-11	0.07	1.5×10^{-19}	0.080	0.441	2.058
CHnv	GU3-14	0.46	2.7×10^{-14}	0.041	1.60	3.872
CHnz	G4-11	0.28	2.0×10^{-18}	0.110	0.308	1.602
PPw	G4-18	0.24	4.5×10^{-16}	0.066	1.41	2.6[illegible]9

[a]Unit designations: TC, Tiva Canyon; PT, Paintbrush; TS, Topopah Spring; CH, Calico Hills; PP, Prow Pass; w, welded; n, nonwelded; v, vitric; z, zeolitized.
[b]S_r is the residual liquid saturation.
[c]α and β are the fitting parameters for the capillary pressure and relative permeability curves, respectively.

low permeability and low porosity (TCw, TSw1, TSw2, and TSw3), and (2) nonwelded vitric tuffs of high permeability and high porosity (PTn and CHnv). The zeolitized nonwelded CHnz has low permeability and intermediate porosity, and the welded PPw has intermediate permeability and porosity. The permeabilities of the nonwelded vitric tuffs are 4 to 5 orders of magnitude greater than those of the welded tuffs and the zeolitized nonwelded CHnz.

Physical properties including porosity, grain density, bulk density at in situ saturation, and dry bulk density have been determined from core samples, and values of these parameters are summarized in Table 3. Additional discussion can be found in Vol. II, Sec. 4.0.

Table 3. Physical and thermal properties of rock in the potential repository horizon.

Parameter	Value
<u>Physical Properties</u>	
Porosity (%)	12 ± 4[a]
Grain density (g/cm^3)	2.55 ± 0.03[a]
Bulk density at in situ saturation (g/cm^3)	2.30 ± 0.09[a]
Dry bulk density (g/cm^3)	2.22 ± 0.10[a]
<u>Thermal Properties</u>	
Dry matrix thermal conductivity (W/m·°K)	2.51 ± 0.17[b]
Dry in situ thermal conductivity (W/m·°K)	2.1 ± 0.2[b]
Saturated in situ thermal conductivity (W/m·°K)	2.1 ± 0.2[b,c]

[a]DOE (1990)
[b]Nimick (1990)
[c]0.65 ± 0.1[illegible] in situ saturation with lithophysal cavities and fractures assumed dry.

On tne basis of samples taken from surface coring, the TSw2 is expected to have 65% saturation (±19%) and a porosity of 15% (DOE, 1990; Klavetter and Peters, 1986). Air in the unfilled voids is expected to be moist although not always at 100% humidity. The observed range in saturation at the repository horizon essentially corresponds to gravity capillary equilibrium (zero net flux). For further discussion see Vol. II, Sec. 1.0.

2.3 Geomechanics

A substantial number of laboratory measurements have been made to determine the mechanical strength of intact samples from the proposed repository horizon. These data indicate that the intact rock is quite strong, with a uniaxial strength of 155 MPa (± 59 MPa) and a high Young's modulus. Uncracked samples have stress-strain curves that show nearly linearly elastic behavior until failure. Samples with cracks exhibit nonlinear stress-strain behavior, as expected when stress is above 50% of the failure stress. Typical stress-strain curves for 50.8-mm-diam saturated samples tested under drained conditions are shown in Fig. 5. Most of the tests for compressive strength have been conducted on samples that were saturated with water and tested under drained conditions. This represents a minimum value, as rocks are generally weaker when saturated with water.

The dynamic properties of the rock are also important, especially in the area of seismic design. These properties include the compressional-wave (P-wave) velocity (C_p), the shear-wave (S-wave) velocity (C_s), the dynamic deformation (Young's) modulus (E_d), and the dynamic Poisson's ratio (v_d). Recommended values of these parameters are given in item 2.2.2 of the RIB as C_p = 3400 m/s, C_s = 2040 m/s, E_d = 23.5 GPa, and v_d = 0.22.

Price (1986) studied the effect of sample size on mechanical properties of Topopah Spring tuff (Tpt) and found that both the ultimate strength and axial strain at failure are inversely related to sample diameter, while Young's modulus and Poisson's ratio are independent of sample diameter. The effect of sample size on ultimate strength is illustrated in Fig. 6.

Estimates of rock-mass strength are based on (1) the known behavior of intact rock, (2) the known joint characteristics, and (3) the presence of applied or confining stresses. A rock-mass strength criterion of

$$(\sigma_1)_{\mathrm{ultimate}} = 16.0 + 10.2\,(\sigma_3)^{0.602}, \quad (1)$$

where $0 < \sigma_3 < 25$ MPa, is presented in item 1.2.6 of the RIB. Equation (1) is based on an assumed rock-mass rating (RMR) of 61 and an unconfined compressive strength of 16.0 MPa.

In situ stress values for the potential repository horizon have been determined from measurements in drill holes USW G-1, USW G-2, and USW G-3 (Stock et al., 1984, 1985). Table 4 shows the average

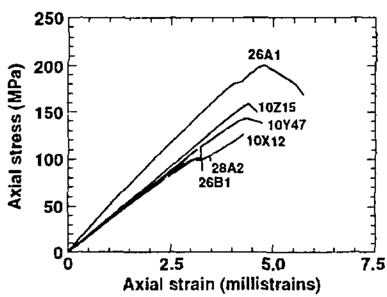

Figure 5. Plots of axial stress vs axial strain for uniaxial measurements on 50.8-mm saturated Topopah Spring tuff samples at 22°C. Measurements were taken at a strain rate of 10^{-5} s^{-1}. Adapted from Price (1986).

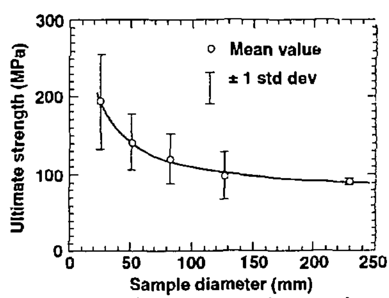

Figure 6. Plot of ultimate strength vs sample diameter for uniaxial measurements on saturated Topopah Spring tuff samples at 22°C. Measurements were taken at a strain rate of 10^{-5} s^{-1}. Adapted from Price (1986).

Table 4. Values and ranges of principal stresses in the potential repository horizon at Yucca Mountain (Stock et al., 1984, 1985).

Parameter	Average value[a]	Range
Maximum principal stress (vertical)	7.0 MPa (1015 psi)	5.0 to 10.0
Ratio of minimum horizontal stress to vertical stress	0.5	0.3 to 0.8
Ratio of maximum horizontal stress to vertical stress	0.6	0.3 to 1.0
Bearing of minimum horizontal stress	N57°W	N50°W to N65°W
Bearing of maximum horizontal stress	N32°E	N25°E to N40°E

[a]Average value for a depth of about 0.3 km (1000 ft).

mean value and range for vertical stress, which is the maximum principal stress and is due to the overburden rock at the site, in addition to the ratios of minimum and maximum horizontal stresses to vertical stress, and the bearings of minimum and maximum horizontal stresses.

In addition, a stress profile for the in situ stress near the ESF has been estimated using a two-dimensional finite element analysis similar to those presented in Bauer et al. (1985), and it can be found in Vol. II, Sec. 4.0 (see Fig. 7 of this report).

3.0 Processes That May Change the NFE

Waste packages will interact with a near field that will be altered from the original conditions by several factors, including construction of the repository, emplacement of waste, and the backfilling of boreholes and/or drifts. All of these can cause chemical changes, possible mineralogical or basic rock mass property changes, as well as hydrologic changes. These changes may be significant relative to the EBS design and performance. However, the changes are very much dependent not only on initial environmental conditions, but also on several other factors such as the specifics of design, operational choices, and repository layout, none of which are well determined at this time. Because of the uncertainties, processes that impact the conditions will be discussed here, with specific changes in conditions identified in Sec. 4.0. The intention of this report is not to give all possible scenarios, but rather, as mentioned previously, to indicate the types of processes that can alter the environment, so that the reader can consider these impacts on the design options.

3.1 Construction

The following discussion includes all activities involved in construction of the facilities that take place prior to emplacement of waste. It does not include construction activities that will take place subsequent to waste emplacement (including closure activities).

3.1.1 Excavation

Excavation activities may enhance both the density and aperture of the fracture system for up to two room-diameters surrounding the openings. The potential for fracture density and aperture modification during preemplacement construction has been evaluated by Sandia National Laboratories (Ehgartner and Kalinski, 1988). They also looked at potential impacts after emplacement and during the retrieval period (50–100 yr). Current understanding of the potential for microfracturing and fracture property changes is that significant changes due to construction are not expected.

Excavation of the shafts, drifts, and boreholes may fracture previously intact rock, and it will expose new mineral surfaces to air. Water in the air will partially hydrate mineral surfaces, although the small moisture content of the air will prevent this process from going to completion.

Excavation of emplacement boreholes and drifts will alter the stress field in the rock near the borehole because the repository horizon is under lithostatic and regional tectonic stress. When sections of the rock are removed, the stress previously supported by the excavated rock is redistributed in the remaining rock. Generally, stress levels and stress gradients near the excavated openings increase and can result in time-dependent deformation of the borehole wall. In addition, the technique used for excavation may affect the mechanical properties of the rock surrounding the excavation. For example, areas that are excavated by the drill and blast technique may contain more fractures in the near field rock than areas excavated using a tunnel boring machine.

Figure 7 shows results of analyses of the impact of ESF excavation on the stresses (DOE, 1990), and Fig. 8 shows the redistribution of stresses around a borehole as a result of excavation (Arulmoli and St. John, 1987). With time, these stress changes will be redistributed. Figure 9 shows the stress redistributions around emplacement

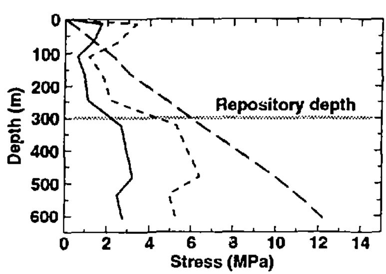

Figure 7. Stress profile along an exploratory shaft near the Exploratory Studies Facility (ESF). The solid line is the minimum horizontal stress, the long dashed line is the maximum horizontal stress, and the short dashed line is the vertical stress. Adapted from the *Yucca Mountain Project Reference Information Base* (RIB) (DOE, 1990).

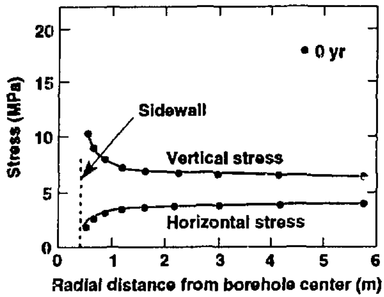

Figure 8. Variation of stress with radial distance from the sidewall at time of emplacement using elastic analysis. These analyses were performed for a 1-m-diam horizontal borehole. Adapted from Arulmoli and St. John (1987).

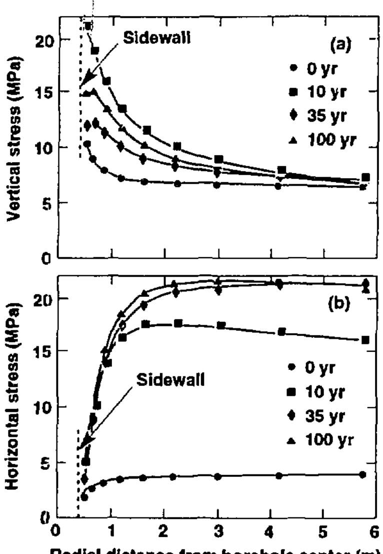

Figure 9. Variation of (a) vertical, and (b) horizontal stresses with radial distance from the sidewall at time of emplacement (as shown in Fig. 8), and at 10, 35, and 100 yr after emplacement. Adapted from Arulmoli and St. John (1987).

boreholes with time (Arulmoli and St. John, 1987). The effect of excavation on the geomechanical properties of rock in the repository horizon has been analyzed for design purposes, and this information is presented in a series of reports published by Sandia National Laboratories (e.g., Johnson, 1981; Johnston et al., 1984; Thomas, 1987). A synopsis of these analyses is presented by Ehgartner and Kalinski (1988). There are no unique issues related to the EBS during the construction period and the reader therefore is referred to Sandia reports on the construction phases.

Other than changes associated with the damaged zone around the excavation, there are no anticipated rock property changes associated with construction.

3.1.2 Drilling and Mining

The introduction of mining and drilling fluids may increase the matrix saturation surrounding the openings. If water is used in drilling or mining, the saturation of the surrounding rock will increase, and fracture flow away from the boreholes will occur. If the drilling fluid is air or air mist, the rock saturation will increase only if the partial pressure of the air/mist is greater than the partial pressure of the moisture held in the pores by the suction potential. If the air is dry, the saturation will be lowered around the borehole. Current plans call for dry drilling and construction so that the likely emplacement environment will be dryer than the ambient or current state.

The impact of a future exploratory drilling operation penetrating an emplacement drift after closure and losing circulation of drilling fluid could introduce enough fluid to maintain a ponded condition for a limited period of time (Buscheck and Nitao, 1991a). Due to the small matrix permeability of TSw2, ponded conditions lasting from days to weeks will only result in centimeters (at most) of lateral imbibition from the fracture into the matrix. Repository mining and drilling operations may result in ponded conditions lasting for a period of days to weeks. Depending on the spacing between fracture networks that are hydraulically connected to the mining/drilling fluid source, several centimeters of wetting front penetration into the matrix may or may not be significant relative to the bulk saturation of the system. Best estimates are that only about 2% of the initially unsaturated porosity along the fractures connected to the source of mining/drilling water would be saturated by the mining/drilling operation.

For welded tuff, Buscheck and Nitao (1988) found that it took about a year for the saturation distribution in the wetting zone along the fractures to nearly equilibrate to background saturation. If the fracture networks at the repository horizon have limited connected path lengths, then the imbibition of mining/drilling will be confined to the scale of the connected fracture path lengths. The experience of Ramirez et al. (1991) indicates that drilling fluids had a negligible impact on the ambient saturation conditions in the vicinity of the G-Tunnel heater.

The most significant impact of the human-intrusion drilling scenario appears to be in driving fracture flow to the WP borehole (thereby possibly entraining radionuclides in a fracture pulse). Of secondary significance will be its effect on increasing the matrix saturation of the near field, thereby enhancing diffusion-controlled radionuclide release modes.

If opening of fractures occurs due to excavation stress relief or redistribution, this will not have any real impact on the WP environment since the effects will be so localized and since fracture-dominated flow is not anticipated during construction, so that aperture or fracture frequency is not important. The only significant changes in hydrologic properties that are expected relate to saturation. The current saturation is depicted conceptually in Fig. 10. Information is insufficient to allow analyses of actual distribution at this time, and, therefore, the conceptual distribution is subject to change. After construction, the rock mass around the WPs will possibly be slightly dryer, as shown in this figure. Drying by ventilation and drilling will not be spatially uniform; therefore, the distribution will be broader, with the mean saturation less than the current 65%.

3.1.3 Mine Ventilation

Mine ventilation may lead to drying of the matrix surrounding the rooms and boreholes. Ventilation of the shafts and drifts will, as noted previously, remove moisture from the rock via evaporation. Salts dissolved in the affected pore water will precipitate, leaving behind a small residue of soluble salts as the pore water evaporates. For those regions where pore water evaporation is incomplete, salt concentration within the pores will be increased, leading to higher ionic strength solutions. This, in turn, will result in elevating the boiling point of pore waters, which

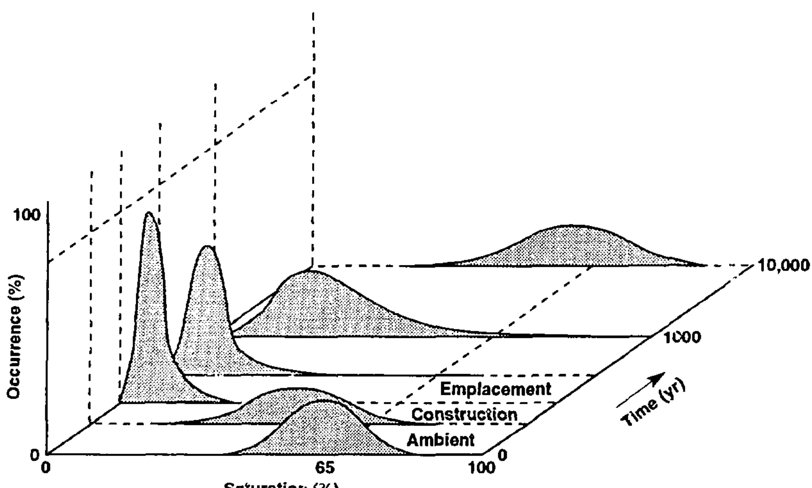

Figure 10. Conceptualization of saturation distribution with time.

may exhibit dry-out. The long term impact (if any) of these salts cannot be determined of this time. The salts may re-dissolve when exposed to water, or they may cause permanent changes in hydrologic parameters. However, the dilute conditions will likely minimize any salt deposition. If wicking occurs with additional deposition of salt, a crust may form similar to cave deposits or to caliche deposits. However, the long time necessary for this to take place, as well as the limited amount of water isolated in fracture-bound blocks, make this unlikely.

The amount of drying caused by mine ventilation will depend on the mine ventilation rates and the duration of ventilation (i.e., time to backfill and closure of the emplacement drifts) and on whether borehole emplacement is used. For borehole emplacement, the extent to which the WP boreholes communicate with the drift (before and after WP emplacement) and the time between drilling a WP borehole and emplacing a WP in that borehole will be important.

3.1.4 Introduction of Man-Made Materials

Man-made materials will be introduced during construction of the facilities. The impact of these materials will not cause significant changes to the preemplacement environment, although some of these materials will become part of the post-emplacement environment. These materials may include such things as engine exhaust, rubber products, metals, and concretes. The major potential for perturbations of the environment due to man-made materials will exist after emplacement, when heat and time will increase the chances for impact on geochemistry of the water.

3.2 Emplacement of Waste

When waste is emplaced, radiation and heat from the waste will cause changes in the environment, which will likely dominate the geochemical/hydrological/mechanical conditions. The material added in the form of waste containers or EBS packing will also have potential impacts on the environment. This section considers the processes that may occur which need to be considered, particularly if these processes are related to design development.

The major cause of hydrologic change is the heat added by the emplacement of waste. This is expected to drive water away from the WPs, which will change the relative hydraulic conductivity, the gas permeability the imbibition characteristics, and other properties of the rock mass. An evaluation of the impact of the emplacement of waste on the hydrologic characteristics must, as a minimum, take into account the changes in saturation. The conceptualization of the saturation conditions of the NFE with time as presented in Fig. 10 is helpful in considering the processes of saturation changes. This figure starts with the expected ambient conditions of 65% (± 19%) saturation. The conceptualization of the ambient conditions is based on the expectation that variability of saturation conditions can be represented by a normal distribution function.

3.2.1 Thermal Loading

Emplaced waste will generate heat as a result of radioactive decay. Thus, waste emplacement will cause a thermal loading of the rock. The thermal loading will decrease with time because radioactivity, the source of the heat, decays with time. Calculations performed for spent fuel 8.5 yr out of reactor core (Fig. 11) indicate that after 100 yr, heat generation is only about 22% of the original emplacement value, although the effects of heating last much longer than 100 yr.

3.2.1.1 Dry Out. After waste emplacement, thermal loading will drive moisture away from waste emplacement openings. Because of the large increase in vapor pressure, nearly all of the air will be driven away from the boiling zone (leaving the gas phase with 100% water vapor). Tests and analyses of the matrix drying show that vapor transport preferentially occurs into openings and along fracture faces. Upon reaching the fractures, most of the vapor is driven away from the boiling zone toward a condensation zone, where it

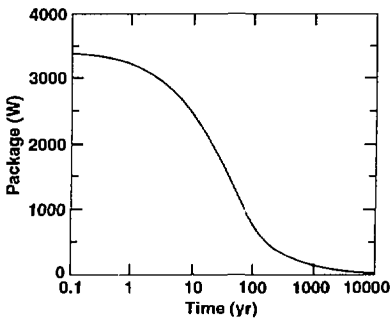

Figure 11. Thermal output of spent fuel (8.55 yr out of reactor core).

condenses and drains down fractures until it is either (1) entirely imbibed by the matrix, (2) enters the saturated zone, or (3) flows back into the boiling zone, where it boils again, forming a "heat-pipe" by refluxing. Low wetting sorptivity of TSw2 appears to facilitate drainage to great depths below the repository. The extent to which condensate drains away from the emplacement zone depends on the competition between gravity drainage and imbibition by the rock matrix.

Figure 12 shows the location of the boiling point isotherm with time. As is apparent, rock will be above the boiling point to considerable distances from the WP. It should be noted that these calculations are made on the basis of young (8.5 yr out of reactor core) and, therefore, initially hot waste emplaced at 57 kW/acre. Emplacement of older fuel at higher APDs will greatly increase the drying and duration of heat effects (discussed in Sec. 4.2).

3.2.1.2 Wetting. As the rock cools below boiling conditions, vapor flow, particularly along fractures, dominates rewetting of the dried-out zone. The dominance of vapor flow on rewetting occurs for saturations between residual saturation and approximately 20%. At very low saturations, below 10%, saturation gradients and the corresponding relative humidity gradients may result in binary diffusion-driven vapor flow from wetter to drier regions, particularly along fractures. For regions of drier rock, which have a larger percentage of smaller pore sizes, capillary imbibition causes this vapor to condense along fracture faces, where it is imbibed by the matrix. Because rewetting is dominated by binary gas diffusion and capillary condensation along fractures, rewetting is

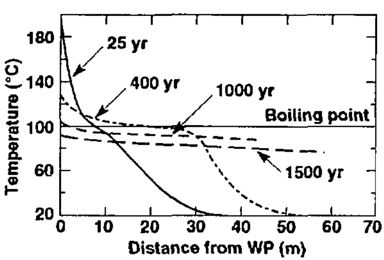

Figure 12. Temperature profiles predicted in the NFE at 25, 400, 1000, and 1500 yr after emplacement of PWR spent fuel (8.55 yr out of reactor core).

strongly dependent on the fracture distribution and connectivity, and it is much less sensitive to fracture aperture and permeability. Until temperature conditions around the WP drop below boiling, the gas phase will be essentially 100% water vapor.

Studies show that rewetting occurs at a much slower rate than drying. This is shown conceptually in Fig. 10, where recovery to ambient conditions does not occur until after hundreds of years, although recent calculations show that for specific emplacement configurations the return to ambient conditions may take hundreds of thousands of years, as shown. The details of emplacement configurations, fuel age, APDs, and operations sequence or other operational considerations will have profound effects on the time of dry out and return of moisture to the WP areas. Design development must take these phenomena into account. Specific scenarios are discussed in the hydrologic properties and modeling sections in Vol. II.

3.2.1.3 Dissolution and Precipitation of Minerals. Hydrologic processes related to drying of the NFE will interact with geochemical processes. In the regions where rock is dried, the processes will be dominated by vapor flow and chemical exchanges associated with vapor flow (Fig. 13). In the portions of this region where temperatures are very near to boiling, the rock will be undergoing drying, with dissolved minerals left in the pores of the rock. This zone may be fairly limited in extent, but the zone will move outward with time so that much of the rock mass may be in this zone at some time. As water is removed, dissolved minerals will be deposited in the throats of pores, particularly the smaller ones. This may result in fundamental changes of the matrix hydrologic properties. One possible effect, if the minerals do not plug the throats but rather restrict them so that they have smaller cross sections, would be to increase the matrix potential beyond values due merely to reduction in saturation. This may be offset by a reduction in permeability. A second possible effect would be totally plugging the smaller pores, so that matrix potential would be decreased. If these salt deposits are irreversible, then permanent changes may take place in porosity as well as matrix potential. Because water in the unsaturated zone is expected to be very dilute, the magnitude of this phenomenon is likely to be small, and it is expected to be reversible. However, increased solubilities due to elevated temperatures may allow redistribution of minerals over long times of heating and cooling. The moisture removed as vapor from this zone will be redistributed,

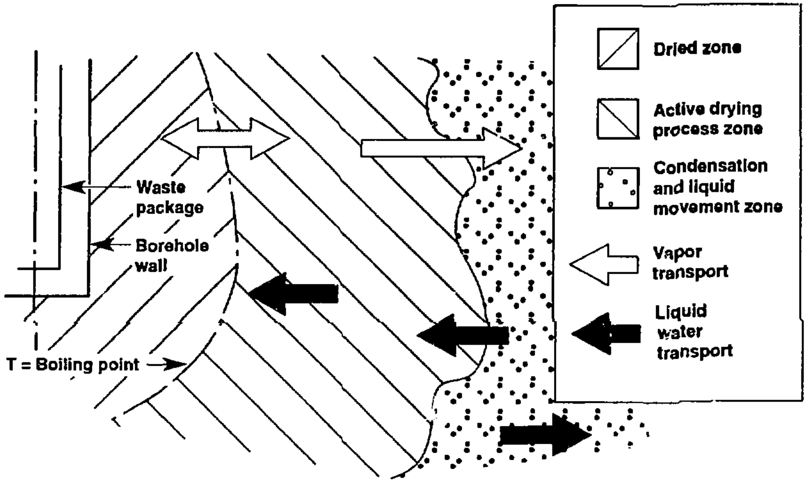

Figure 13. Geochemical/hydrological zones. The dried zone has no liquid water and therefore only vapor geochemical processes. The active drying process zone has lower saturation (more concentrated fluids) with a tendency for liquid flow due to saturation gradients. Elevated temperatures create potential for increased chemical reaction rates. Increased concentrations and decreased saturation restrict chemical reactions. There is potential precipitation in this zone. The condensation and liquid movement zone has increased water available at elevated temperatures and thus potentially increased chemical activity.

possibly in a condensation zone where both saturation and temperatures are elevated above ambient (Fig. 14).

The zone of rock where temperatures are elevated, but are below the boiling point, will be very active both hydrologically and geochemically, with potential for active dissolution and precipitation of minerals. Numerous experiments have demonstrated that the chemical composition of the water is likely controlled by the solubility of mineral phases present in the rock (Knauss, 1987; Knauss and Peifer, 1986; Knauss et al., 1986). As the water interacts with the rock, dissolution of minerals present in the rock will occur, along with formation of new secondary minerals. The rates of the controlling dissolution and precipitation reactions are such that equilibrium will be approached on the time scale of months to a few years. The secondary minerals that form include clays and zeolites; the particular assemblage of minerals that forms depends upon the temperature of the environment. Laboratory work indicates that healing of fractures can occur in this region (see Fig. 15) (Lin, 1990).

In the condensation zone, the water deposited as condensate will be essentially distilled and may not be in chemical equilibrium with the rock matrix. Because of the elevated temperatures, it is possible that this zone will be one of increased geochemical activity. Because this is not a stationary zone, that is, the boiling and condensation fronts move out from the WPs with time until some time after the repository horizon temperatures begin to decline, the time for geochemical reactions to take place will vary from one location to another. The extent or significance of the geochemical reactions are not currently fully understood.

3.2.1.4 Increased Stress. The largest effect on the geomechanical behavior of the NFE is expected to be due to the thermal cycle, in which the rock will be rapidly heated and then allowed to slowly

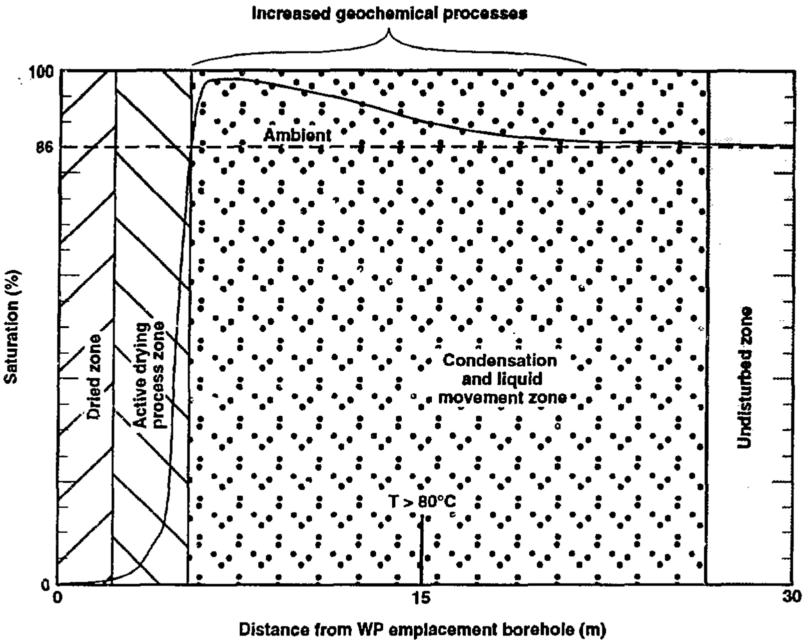

Figure 14. Saturation conditions of the near field for a 25-yr postemplacement spent-fuel canister. The dry-out condensation curve is shown for 8.6-yr-old spent fuel. Increased geochemical processes occur in the condensation and liquid movement zone, where an increased volume of water is available at elevated temperatures. Note $T > 80°C$ at 15 m.

cool. The thermal loading of the NFE will alter the stress in the rock near the emplacement openings (borehole or drift) as a function of time. During the period of temperature increase, the stress in the near-field rock will increase as the rock tries to expand. However, due to geometry of the excavated drifts (and boreholes, if used), the stress fields in the NFE will be complex, and some zones may even be put in tension for an extended period of time. As the temperature decreases, the overall stress levels will decrease, and the entire stress will again be compressive. Several studies have been done to estimate the stress distribution and geomechanical behavior of the rock in the repository due to heating. Many of these studies have focused on the rock response around emplacement boreholes over a time period of 100 yr. Results indicate that overall, the boreholes should be stable and that stresses may remain at levels in the range of 20 to 40 MPa for well over 100 yr. Estimates have not been made that include the thermal cycle of heating and subsequent cooling of the geomechanical behavior of the rock around the emplacement hole, incorporating time-dependent rock properties, for periods greater than 100 yr.

While it is not expected that radiation will have major impacts on the geomechanics, sufficient studies to address these issues have not been conducted at this time. However, this lack of information doe not represent a major risk since the potential effects of the uncertainties can be mitigated by EBS design options.

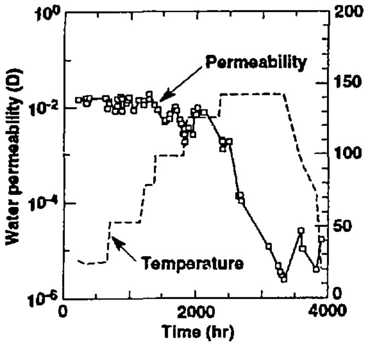

Figure 15. Water permeability and temperature as a function of time on a Topopah Spring tuff sample with a saw-cut fracture.

3.2.2 Radiation

Emplacement of waste will also impose a radiation field upon the rock in the NFE. The effect of radiation depends on the design selected. If there are self-shielded containers, then the effects will be minimal. If the borehole or drifts are dry, very minor changes to the geochemistry are anticipated even with a thin-walled reference WP in a vertical borehole. The only potential effects would be to the rock itself because a few cm of the rock effectively shields radiation so that it will not interact with pore water or water in fractures. The effect of radiation on the geomechanical properties of rock from the potential repository horizon has not been determined. However, radiation is expected to have a negligible effect on the geomechanical behavior. This supposition is based on the work of Durham et al. (1986), who conducted a series of unconfined compression tests on cylinders of quartz monzonite, half of which were irradiated with gamma radiation and half of which were not. A similar series of tests were conducted by Durham et al. on samples of Westerly granite. These experiments showed no statistically significant change in unconfined compressive strength for either rock type. Null results were also found for the effect of gamma irradiation on Young's modulus and Poisson's ratio. Durham et al. concluded that gamma irradiation has no effect on the strengths of either rock type. A similar series of tests are proposed for rock from the repository horizon, and similar results are expected.

3.3 Closure

Major activities associated with closure that might impact the environmental conditions include (1) ceasing of ventilation, (2) emplacement of seals in openings, (3) the introduction of construction materials, and (4) removal, if any, of shaft and drift support systems.

The effects of ceasing of ventilation would depend on how the repository is operated. For example, if panels are filled and then ventilation is shut off in panels that are filled, the effect of ceasing ventilation at closure would be minimal. The effects would be even less if after emplacement in panels is completed some sort of barrier or door were placed across drift entrances.

The emplacement of seals in openings would potentially impact the chemistry of the NFE. They would also potentially impact the vapor and water flow paths in the rock mass. Further, they would permanently alter any natural or nonforced ventilation of the underground workings.

The largest possible impact of the introduction of construction materials would probably be the introduction of fluids, especially water in grout or concrete used, or introduction of materials that could cause chemical changes in the NFE (see Sec. 3.1.4)

The removal of shaft of drift support systems could change the flow paths for fluids or gases. It could also impact block stability or geomechanical conditions.

3.4 Backfilling

Environmental conditions most likely to be impacted by backfilling include the hydrologic characteristics and an early transient thermal effect of different heat conduction in the backfill than in the rock mass. Backfilling will also influence opening stability, but that is a design related issue, not an environmental characteristic.

It is likely that backfill materials will be the tuff removed during excavation. Excavated materials will either be temporarily stored in drifts, where it is assumed there would be some sort of dust control by ventilation, or on the surface. The moisture in the excavated materials would be reduced because ventilation air and surface conditions are expected to be considerably drier than the in situ rock saturation conditions. With handling and breaking of rock, this drying process would be facilitated. Thus, backfill will likely have lower saturation than the original rock-mass saturation. However, backfill will possibly have greater saturation than the dried-out rock mass unless the backfill materials have been stored in areas of drifts that were above the boiling point of the rock. Once emplaced, the backfill will act as a porous medium that, depending on the material chosen, could disperse any episodic fracture-dominated flow and modify thermal conditions since the thermal conductivity of granular backfill will be lower than for intact rock.

The thermal conduction of the backfill will be lower than that of the rock-mass because of the porous nature of the backfill (assuming that the backfill consists of crushed tuff).

3.5 Climate or Site Environment Changes with Geologic Time

Hydrologic discussions for the NFE included in this report assume that conditions will remain unsaturated for the 10,000-yr performance period. They do not address changes that can take place during the 10,000-yr time frame that might affect the overall hydrology of the site (e.g. climatic changes). The evaluation of the potential for these types of changes (particularly climate or seismic) to occur sufficient to change the unsaturated character of the site is not complete. Therefore, evaluation of any potential impacts on the WP is left for future studies and will be reported in revision of this document. However, preliminary information is included that addresses how sensitive the hydrologic response might be to differing flux conditions. The flux at the depths of the NFE is very much dependent on the response of the overlying units. Predictive model results are not available that address the potential for climatic changes, nor what impact any changes would have on the flux within the repository horizon.

4.0 Postemplacement NFE

4.1 Mechanical Loading Conditions

Under assumed conditions, there should be no rock loading on the WPs. There is no contact between the WP and the rock mass in the current reference design. If there are borehole failures with time, then the WP can be loaded by contact with the rock. The failure mechanisms that could lead to loading of the container include (1) block failures, wherein blocks could fall into the borehole, (2) rock mass failures, where caving of openings or rock bursts (unlikely) may occur, (3) creep, in which the openings close onto the package, or (4) sloughing of materials into the openings. The type of loadings that would result from these failures will be different and are assessed separately in the following sections.

It should be noted that if significant effects occur, they can be mitigated by engineered alternatives such as borehole or drift liners, or other EBS components. The effectiveness of some engineered approaches would be greater during the preclosure period, which is more in keeping with the durations typical of engineering experience. However, some alternatives such as drift backfill should remain effective against drift collapse indefinitely. Even if settlement of backfill occurred, the amount of rock motion would be limited.

Kemeny and Cook (1990) used a probabilistic approach that included time-dependent crack growth to evaluate stability. They estimated that over the lifetime of the repository, slabbing is likely to occur in a significant portion of the emplacement boreholes. Slabs could place either uniform or point loading on the WPs or on liners, etc.

4.1.1 Uniform Loading

Uniform loading could result from creep closure of openings or from very small rock fragments entering into the openings. If sufficient long-term creep takes place to entirely close the openings around the WPs, then the full lithostatic load might be imposed. While data are not available to address creep over the long time frames (10,000 yr), there is no indication that the full lithostatic loading is likely to be imposed. Natural openings in other rock types have remained open over long periods of time (e.g., limestone caves and lava tubes), but no study has been made as to whether these natural analogues can apply to Yucca Mountain.

The second possible mechanism for uniform loading, wherein sloughing of rock materials into the openings occurs such that the opening is filled by sloughed materials, is more likely to occur but probably will not result in the entire lithostatic loading conditions on the WP. Unless sloughing occurs with sufficient mechanisms to tightly pack the opening or subsequently compress or compact the slough, these sloughed materials will not transmit the lithostatic loading conditions. A combination of sloughing and rock creep or block failure would be required to impose the lithostatic loading across the sloughed rock materials.

A third mechanism for uniform loading is hydrostatic loading. No hydrostatic loading is anticipated since the repository horizon is unsaturated. Any water that might be introduced inadvertently into the system will likely drain away before any appreciable head can develop. Therefore, no hydrostatic loads need be provided for.

The above conditions are very dependent on the design used. For instance, both sloughing and creep are most likely to occur during the high temperature phase of disposal. If a liner or other support is provided to prevent movement of materials into the openings, then the likelihood of their impacting the WP would be greatly reduced. To some extent, this is also true of block failures, although block failures are more likely after the heat effects have peaked and temperatures have returned to ambient conditions.

4.1.2 Point Loading

The most likely means of creating point loadings would be either block failures or tipping of the WP. Loads imposed by tipping would depend on whether there were accompanying rock movements such as block or creep. If there were no loads imposed by rock failures or deformations, then point loading would be limited to loads imposed by the WP itself.

The size of blocks that could enter into an emplacement borehole is dependent on the fracture spacing and, ultimately, on the opening dimensions. For horizontal emplacement, it is conceivable that vertical joints with different orientations could form a block with dimensions of about 1 m^2

horizontal dimension that could extend for some considerable distance vertically. Given the dry bulk density of 2.22 g/cm^3, this would be equivalent to ~2000 kg/vertical ft of block. A reasonable estimate for point loadings by a tabular block can be made by using a ratio of 10:1 vertical to horizontal dimensions for the block. At vertical dimensions greater than 10:1, an estimate of the locking into the overall fracture/block system needs to be made. For vertical emplacement, a reasonable estimate can be based on a block of dimensions roughly the size of the opening. Thus, a block of about 1 m^3 could be used to make the assessment.

The above estimates assume that the blocks break free from the rock mass and do not have any loading applied to them from the remainder of the rock mass. In reality this is not likely to be the case, and a detailed key block type analysis will be needed to assess the actual loading expected. This type of analysis has not been performed to date.

4.1.3 Seismic Loading

Earthquakes and distant underground nuclear events (UNEs) generally affect the NTS underground excavations through either fault slip or shaking. Damage due to fault slip will occur when the emplacement drift or borehole passes through a fault zone. Under such circumstances, damage is generally restricted to the fault zone, and it may range from minor cracking of a tunnel liner to collapse of a portion of the excavation, depending on the fault displacement and the engineering properties of the NFE. If an emplacement borehole or drift is found to cross an active or potentially active fault zone, that emplacement borehole or drift and the nearby host rock region will not be used for waste emplacement.

Excavation damage as a result of shaking or vibratory motion has been widely investigated. For unlined underground excavations in rock, such damage occurs as rock fall, spalling, local opening of rock joints, and block motion. Subramanian et al. (1990) have provided recommendations for seismic parameters for the design of the shafts associated with the ESF. These are summarized in Section 2.1.1 of the RIB. The recommendations include design parameters for both natural earthquakes that may occur at or near the repository site and for UNEs that may occur at the Nevada Test Site (NTS).

The Bare Mountain fault, located 16 km west of the ESF, appears to be the most likely source of potentially severe ground shaking. A magnitude 6.5 earthquake on the Bare Mountain fault was used as the deterministic basis for establishing the earthquake ground-motion condition, based on the probability that this fault has an average Quaternary slip rate of up to 0.15 mm/yr (Subramanian et al., 1990). Other faults exist in the area, such as the Amargosa Valley of the stateline-Pahrump Valley-Stewart Valley fault zone, but these were not considered in the design basis calculations. The design-basis UNE was a 700-kt weapons test at the closest practical point in the Buckboard area of the NTS (described in Vortman, 1980).

Recommended surface control motion values for the natural earthquake design are 0.30 g horizontal acceleration and 30.0 cm/s peak horizontal velocity (Subramanian et al., 1990). Subramanian et al. recommend the use of control motions 1.67 times these design-basis values for performance evaluations of the ESF. Factors that influence ground motion include source magnitude, distance, and type; rupture dynamics; transmission path effects; and site geology. The first two factors (source magnitude and distance) are considered the most important. Peak horizontal acceleration and velocity for the design-basis earthquake were extrapolated from recent observational data combined with other considerations. Similar engineering judgement was used in recommending vertical, radial, and transverse component values.

The prediction of peak ground motion of the design-basis UNE was done using empirical equations that were based on measured ground motions from a number of UNEs conducted in the Pahute Mesa area of the NTS (Table 5). An evaluation of the data indicated that observed ground motions were greater than previously predicted but within the accuracy limits of the prediction equations. Conservative estimates of design-basis UNE motions were determined for a nonexceedance probability of 95%. Median predicted values and recommended motion parameters for the design-basis UNE are given in Table 5.

Subramanian et al. further recommend that for design purposes, and until site characteristics are better quantified, surface-control motion values apply at all depths (i.e., no attenuation of ground motion with depth is assumed).

Attempts to catalogue records of the performance of underground excavations subjected to seismic loading and develop simple empirical design criteria have indicated a damage threshold of approximately 20 cm/s (8 in./s). No damage should be experienced if the peak particle velocity is beneath that threshold. It is important to note,

Table 5. Recommended motions for the design-basis UNE (Subramanian et al., 1990).

Component	Median predicted value	Design-basis UNE values [95% nonexceedance level (1.65 σ)]
Vertical acceleration (g)	0.05	0.2
Radial acceleration (g)	0.03	0.1
Transverse acceleration (g)	0.03	0.1
Vertical velocity (cm/s)	4	9
Radial velocity (cm/s)	4	12
Transverse velocity (cm/s)	3	12
Vertical displacement (cm)	1	2
Radial displacement (cm)	1	3
Transverse displacement (cm)	1	4

however, that ground motion resulting from earthquakes can last for several seconds, subjecting the excavation to repeated stress cycles; the number of stress cycles is critical to determining how much permanent deformation will occur within a rock mass around a tunnel when subjected to earthquake loading.

Kana et al. (1989) recently reviewed the literature on seismic loading for an underground repository and found that because studies completed to date have ignored both time-dependent fracture properties and the duration of shaking, they are of limited use in predicting the rock response to seismic loading by earthquakes. They conclude that further investigation is needed to resolve this issue.

4.2 Thermal Effects of Waste Emplacement

Temperatures of the repository/NFE will depend on total mass loading of the waste. Table 6 shows temperatures calculated for various loading scenarios. Figure 16 shows temperature profiles for the repository centerline that result from emplacement of 30-yr-old spent fuel at the current reference loading of 57 kW/acre. As noted, the rock around the WP will peak around 113°C. Figure 17 shows the edge effects for the repository. As noted, the edge effects are not pronounced, and, further, the peak temperatures do not extend very far beyond the repository. Figure 18 shows that the temperatures are dependent on APD for a given spent-fuel age.

The temperatures may also depend on hydraulic flux. Long-term near-field calculations were conducted for surface recharge fluxes of 0.1, 0.5, and 1.0 mm/yr. Tables 7 and 8 summarize the three cases that have fluid flow. Figure 19 shows a comparison of the temperature history of the WP for different fluid fluxes. The effect of the surface recharge rate is relatively small. The temperatures for the cases that included fluid flow in the pores, as opposed to the case where only thermal conduction was considered, are significantly lower after the first 20 yr. This is due to boiling of liquid, which then condenses away from the boiling zone and refluxes, resulting in the increased heat transfer. This is in essence a naturally occurring, gravity-driven "heat-pipe" phenomenon.

Chemical changes may take place as a result of the increased temperatures and associated drying process. These chemical changes may result in permanent changes in hydrologic properties. Specifically, porosity, hydraulic conductivity, and matric potential may be altered due to deposition of minerals within the pores as a result of drying. Also, fracture healing may result from mineral dissolution/deposition associated with heating/drying processes, which would impact the potential for fracture flow.

4.2.1 Changes in Rock Properties

The thermal properties of rock samples from the proposed repository horizon have been the subject of several laboratory and field studies. Results indicate that the dry matrix thermal conductivity is 2.51 ± 0.17 (W/m·°K). The in situ

Table 6. Repository temperatures calculated for various loading scenarios.

Spent-fuel age (yr)	Areal power density (APD) (kW/acre)	Peak drift-wall temperature (°C)	Drift-wall temperature at repository center (°C)		
			100 yr	1000 yr	5000 yr
10[a]	57	200	180	110	—[b]
30	20	60	60	57	38
	36	90	90	84	49
	40	96	96	89	51
	57	122	119	110	62
	72	143	137	127	72
	80	153	147	134	76
	100	180	170	163	88
	114	225	200	184	95
	160	283	283	219	121
60	57	147	132	138	82
	114	270	241	230	131

[a]Reference case is vertical emplacement. All other cases considered are drift emplacement.
[b]Less than 100°C at 2600 yr. Calculations not carried out to 5000 yr.

Table 7. Initial conditions in rock adjacent to the WPs for different surface recharge rates imposed at the ground surface.

Surface recharge rate (mm/yr)	Gas-phase pressure (Pa)	Initial bulk saturation, S_{bi} (%)	T (°C)
0.1	1.026×10^5	85.4	23.18
0.5	1.026×10^5	98.0	23.14
1.0	1.026×10^5	98.5	23.09

thermal conductivity has been measured both dry (2.1 ± 0.2 W/m·°K) and at a saturation of 0.65/2.1 ± 0.2 W/m·°K.

In addition, the effect of temperature on the strength of near-field rock is not well defined at this time. Rock strength, however, generally decreases with increasing temperature. Price et al. (1987) report that for samples from the potential repository horizon, Young's modulus decreases an average of 16% as temperature is raised from 22 to 150°C. The mean ultimate strength also decreases 16% as temperature is raised from 22 to 150°C at both 0 and 5 MPa confining pressures.

Table 8. Summary of hydrothermal conditions at the WP and the borehole wall (BHW).

Surface recharge rate (mm/yr)	S_{bi} at BHW (%) (See Table 7)	Time for $S_b \geq 0.10$ at BHW (yr)	Time for $S_b \geq S_{bi}$ at BHW (yr)	T_{max} of WP (°C)
0.1	85.4	1400	>2600	202
0.5	98.0	1000	>2600	199
1.0	98.5	1000	>2600	199

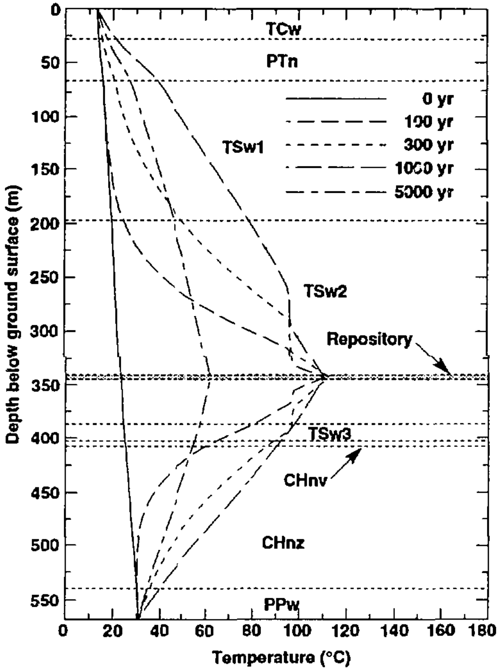

Figure 16. Vertical temperature profiles along the repository centerline for 30-yr-old spent fuel, an APD of 57 kW/acre, and zero recharge flux. The profiles are flattened at the boiling zone (≈96°C), and the temperature disturbance reaches the ground surface within 300 yr.

Measurements of linear thermal expansion have been made on samples from unit TSw2, and Table 9 presents the coefficients of linear thermal expansion. The values represent coefficients of linear thermal expansion during heating; and the coefficients shown for the intact rock should be used for calculations that do not involve very near-field regions. Coefficients of linear thermal expansion during heating for very near-field regions are also shown. These apply only to welded, devitrified tuffs that are close to or at a free surface and are in an initial stress state that is essentially unconfined. It is important to note that these coefficients should not be used for calculations of displacements or stresses during cooling; thermal expansion behavior is hysteretic and depends on the maximum temperature reached by the material. Coefficients of linear thermal expansion are assumed to be identical for both intact rock and the rock mass.

Thermal capacitance has also been estimated for unit TSw2 for various temperatures and values listed in Table 10 and Fig. 20.

Phase changes may occur in some minerals which can cause step changes in the rock volume. A specific example is cristobalite. This mineral exhibits a few percent volume increase in transition from alpha to beta phase, which occurs at temperatures around 200°C. However, cristobalite is expected to represent only about 10% of rock mass volume, and depending on desig. less than 15% of the rock volume will be elevated to temperatures

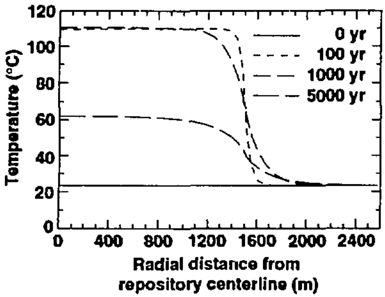

Figure 17. Radial temperature profiles at the repository horizon for 30-yr-old spent fuel, an APD of 57 kW/acre, and zero recharge flux. Note that temperatures are uniform within the inner two-thirds of the repository.

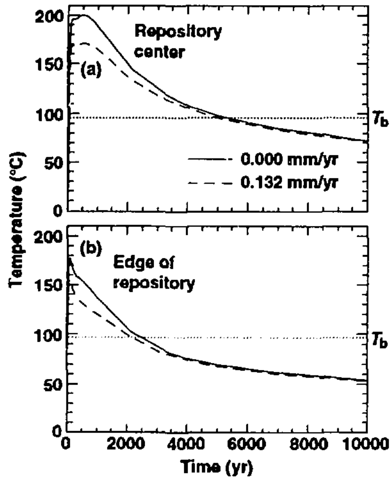

Figure 19. Temperature histories calculated for two widely different recharge fluxes (0.000 mm/yr and 0.132 mm/yr) at the (a) repository center, and (b) edge of the repository. The duraticn of boiling conditions is relatively insensitive to the recharge flux and initial saturation conditions. P. ofiles are for 30-yr-old spent fuel and an APD of 114 kW/acre.

approaching 200°C. The phase change, if it does occur, is reversible, so that a volume decrease would occur upon cooling below 200°C.

4.2.2 Changes in Hydrologic and Geochemical Properties

Figure 4 shows the suction potential of intact Topopah Spring tuff samples at 70°C. Data at 70°C show that the saturation at the same suction potential decreases with increasing temperature. This is expected because the surface tension of

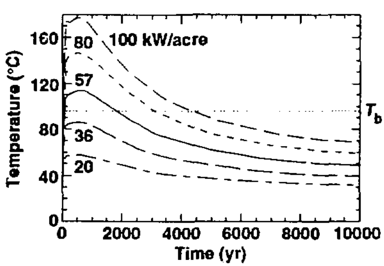

Figure 18. Temperature history at the repository center for 30-yr-old spent fuel and zero recharge flux. For spent fuel of a given age, the temperature rise is proportional to the APD. Note that the nominal boiling point (T_b = 96°C) is shown for reference.

water decreases with temperature. It is also shown that the hysteresis of the characteristic curves is smaller at 70°C than at 20°C. Measurements of suction potentials at temperatures greater than 70°C have not been made. These measurements will be made in the future; however, there is a practical limit of 100°C, at which point water boils (unless under unrealistic pressures) and there is no suction potential.

Laboratory studies indicate that, under specific conditions of flowing water or steam and confining pressures, water permeability of a fractured tuff sample depends strongly on temperature. A decrease in water permeability has been measured in the laboratory for temperatures >90°C. The decrease in water permeability continued when the temperature increased. Dehydration and rehydration were not required to ensure the decrease of permeability. The presence or absence of secondary minerals on the fracture surfaces had

Table 9. Coefficients of linear thermal expansion (10^{-6}/°C) for unit TSw2 during heating.

	Temperature range (°C)																	
	25–50°			50–100°			100–150°			150–200°			200–250°			250–300°		
Type	$\bar{\alpha}$	σ	n	$\bar{\alpha}$	σ	n	$\bar{\alpha}$	σ	n	$\bar{\alpha}$	σ	n	$\bar{\alpha}$	σ	n	$\bar{\alpha}$	σ	n
Intact rock	9.1	1.3	9	8.2	0.8	9	6.8	0.5	4	9.7	—	1	—	—	—	—	—	—
Very near field	5.4	2.2	12	8.0	1.5	12	9.8	1.7	12	17.0	11.6	12	25.0	15.7	11	35.6	10.8	7

$\bar{\alpha}$ = mean coefficient of linear thermal expansion.
σ = standard deviation of the sample group.
n = number of samples analyzed.

no effect of the decrease of permeability. The roughness of the fracture surfaces had an effect on how the permeability decreases but had no effect on the total decrease of permeability, as shown in Figs. 21 and 15. When the temperature was decreased to room temperature, the permeability did not recover to its pre-heat-treated values.

Analyses indicate that both dissolution and deposition of silica minerals can occur on the fracture surfaces during the flow of water. Other mechanisms may also affect the decrease of permeability of a fractured sample, such as deformation of the fracture surfaces due to temperature and confining pressure. However, tests have shown that for dry samples, temperature and confining pressure do not cause decreases in permeability (Fig. 22). Apparently, water is required for a decrease of permeability of a fractured Topopah Spring tuff sample. These tests also indicate that flowing water and sample temperatures greater than 90°C seem to be required to cause the decrease of permeability. Figure 23 shows the effect of flowing steam on gas permeability. The gas permeability after flowing steam through the fractured sample decreased by more than one order of magnitude.

Table 10. Values of rock-mass thermal capacitance for unit TSw2 at selected temperatures (DOE, 1990).

Temperature (°C)	*Thermal capacitance* (J/cm³K)
25	2.0324
50	2.1280
94	2.2638
95	10.7683
105	10.4690
114	10.1984
115	2.0065
155	2.1114
195	2.1912
235	2.2692
275	2.3410

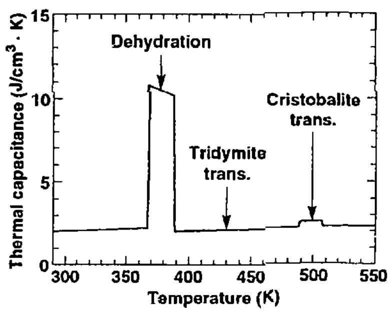

Figure 20. Rock mass thermal capacitance of unit TSw2, showing the effects of dehydration and cristobalite transformation. The temperature of trydymite transformation is shown for reference. Adapted from the *Yucca Mountain Project Reference Information Base* (RIB) (DOE, 1990).

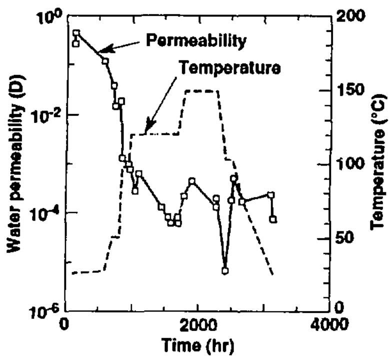

Figure 21. Water permeability and temperature as a function of time on a Topopah Spring tuff sample with a tensile fracture.

There are at least two possible mechanisms for decreasing permeability: smoothing of the asperities of the fracture surfaces due to the dissolution and deposition of minerals on the fracture surfaces, and decreasing of the fracture aperture due to water or steam-weakening of the asperities of the fracture surfaces, which allowed for closure under the confining pressures applied during the tests.

Conditions conducive to fracture healing may exist at Yucca Mountain subsequent to waste emplacement, when steam and condensate at elevated temperatures flow through the fractures. However, the laboratory tests that identified fracture healing were performed at very high pore pressures and water volumes, both of which exceed those expected at Yucca Mountain by perhaps orders of magnitude. Further, a decrease in permeability was not observed during prototype field testi.g at G-Tunnel (Ramirez et al., 1991). The performance implications if permeabilities

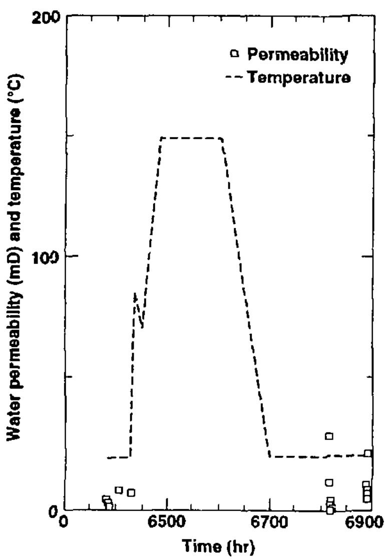

Figure 22. Water permeability of a naturally fractured Topopah Spring tuff sample measured at 20°C before and after heating to 150°C with standing water in the sample.

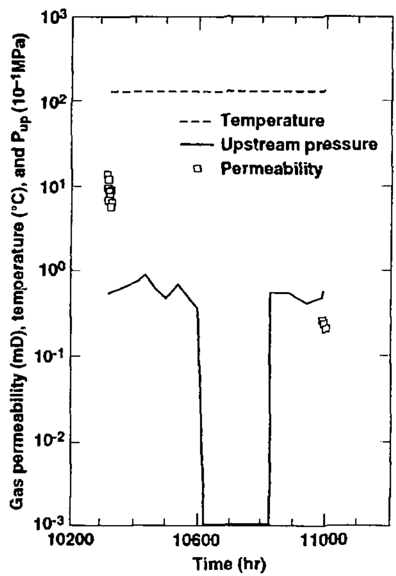

Figure 23. Gas (N_2) permeability of a dry, naturally fractured Topopah Spring tuff sample measured at 127°C before and after flowing steam through the sample.

decrease are dependent on the scenario under which the decreases occur. If the decreases occur after the rock mass is dried out, then the implications are positive since the fracture healing would prevent water from entering the waste emplacement openings. If the healing takes place before the water is removed, then performance may be adversely impacted since this water will remain in the system, where it may contact the WPs.

4.2.3 Dry-out

As a result of the emplacement of waste, rock mass temperatures within the NFE will be elevated, possibly above the boiling point of water (depending on the configurations and designs of the EBS and repository and the mass density of emplaced waste and age of the waste). If the temperatures exceed the boiling point, boiling and rock mass dry-out will result in (1) a dry-steam environment around the waste during periods when the temperatures remain above the boiling point, and (2) dried-out rock mass (lower degree of saturation), which will inhibit flow of liquid water through the dried rock, thus minimizing water contact with the EBS.

As the heat from the waste dries out the rock surrounding the WPs, a significant volume of the water will be removed from the WP environment. The amount of water depends on the preemplacement moisture content of the rock mass, the amount of heat, the age of the fuel, and the emplacement configuration. Figure 24 shows the volume of water removed for different APDs

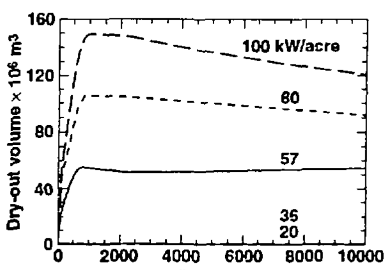

Figure 24. Dry-out volume of liquid water vs time as a function of emplacement APD for 30-yr-old spent fuel and zero recharge flux. The threshold APD for significant dry-out by boiling lies between 36 and 57 kW/acre.

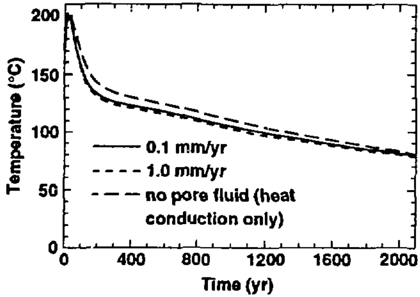

Figure 25. Borehole surface temperature for steady-state recharge fluxes of 0.1 mm/yr, 1.0 mm/yr, and no pore fluid (heat conduction only) for 2000 yr. Calculation is for 8.6-yr-old spent fuel with an APD of 57 kW/acre.

considering 30-yr-old fuel and zero recharge flux, which is our best estimate of the flux at the repository level. These calculations show that between 36 and 57 kW/acre is the APD threshold for creating significant dry-out for 30-yr-old spent fuel. Figure 25 shows that temperatures, and thus dry-out, are largely insensitive to recharge flux. Figure 26 shows the impact of 30- and 60-yr-old fuel on the volume dried out. Dry-out conditions can persist for long periods of time. Figure 27 shows that the persistence of dry conditions may extend beyond 10,000 yr.

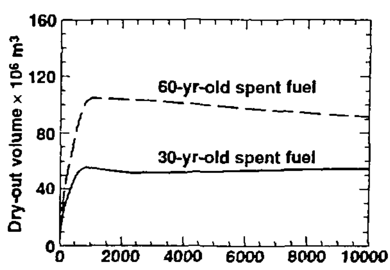

Figure 26. Dry-out volume of liquid water vs time for 30- and 60-yr-old spent fuel emplaced with an APD of 57 kW/acre, and zero recharge flux.

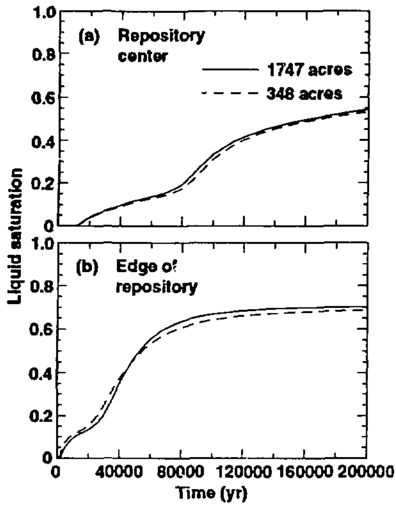

Figure 27. Liquid saturation with time at the (a) repository center, and (b) edge of the repository for 60-yr-old spent fuel and an APD of 114 kW/acre. Dashed lines indicate temperatures if the spent-fuel volume is the same as that of the reference design, and the repository area decreases because of the higher APD. Solid lines indicate the reference design repository area with increased spent fuel to account for an APD of 114 kW/acre.

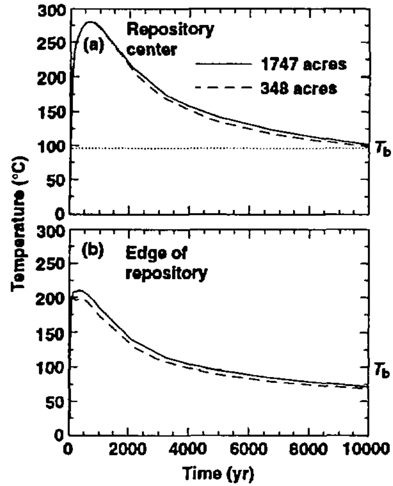

Figure 28. Temperature histories vs time for the (a) repository center, and (b) edge of the repository for 60-yr-old spent fuel, an APD of 114 kW/acre, and zero recharge flux. The duration of boiling conditions is relatively insensitive to repository size.

Figure 28 shows that for 60-yr-old fuel and 114-kW/acre APD, dry steam conditions can persist for more than 4000 yr at the repository edge or over 10,000 yr for the center of the repository. As can be seen in Fig. 24, dry-steam conditions will persist for thousands of years for all APDs above 57 kW/acre. As shown in Fig. 25, dry-steam conditions can be maintained for over 12,000 yr for the reference case of 8.5-yr-old waste at 57-kW/acre APD. As noted, the length of time that dry-steam conditions can be maintained can be extended if old waste at high APDs is emplaced. This results from the lower rate of thermal decay for older waste, which results in long term APDs that more closely match the emplacement APDs. As can be seen in Table 11, there is a considerably greater percentage change in thermal load of 10-yr-old spent fuel as it ages than for spent fuel that is 100 yr old at the time of emplacement.

4.2.4 Rehydration

The work performed at the G-Tunnel prototype test (Ramirez et al., 1991) also indicates that

Table 11. Percent of emplacement thermal load remaining at 100, 1000, and 10,000 yr as a function of age of waste at time of emplacement.

Age of waste at emplacement[a] (yr)	Percentage of emplacement thermal output		
	100 yr	1000 yr	10,000 yr
10	27	0.8	0.2
30	36	1.2	0.3
60	43	1.7	0.4
100	57	2.9	0.7

[a]If waste is aged in place, emplacement age would be equivalent to age at time of closure or final loading.

the time for rehydration of the rock once it has been dried out is longer than the time for the original dry-out. The elevated temperatures will raise the partial pressure of the water, and so it is likely that the environment will remain dry for a considerably longer period than that period when the temperatures exceed the boiling point. These conclusions are moderated by the observation that much of the rehydration may take place by binary diffusion for saturations less than 10 to 20%. Evaluations of flux conditions at the repository level using ECM approaches indicate that there is essentially zero flux within the repository horizon tuffs. This analysis appears to be consistent with saturation measurements. If this is an accurate assessment of the flux, then once the water is removed from the system by gravity drainage along fractures below the waste horizon, there is no source of water to rehydrate the matrix. Therefore, if flux conditions remain as they are at present, it is possible that the saturation will not return even after the temperatures decay except by the extremely slow process of capillary imbibition from the water table, which will rewet the matrix.

The dry conditions are shown conceptually in Fig. 10 where, for the SCP reference case of 57 kW/acre 10-yr-old waste, the waste emplacement environment will be essentially dry for at least 300 yr and will likely continue to be dry for more than 1,000 yr, both as a result of the unsaturated ambient conditions and thermally induced drying. As the heat generated by the waste dissipates, there will be a gradual return to ambient (65%) saturation. Dry conditions are favorable to the waste container and waste-form performance because (1) corrosion by liquid water is the most aggressive environment for the container, and (2) leaching by liquid water is the most likely mechanism for release and transport of radionuclides from the EBS.

Figure 29 gives the time history of the liquid saturation in the rock next to the borehole face. Water first returns to the WP environment because of steam in the gas phase moving towards the WP and condensing at temperatures higher than the nominal boiling point due to capillary condensation (vapor pressure lowering). This phenomenon only occurs at liquid saturations below about 0.1, where the capillary tension is sufficiently high. The high capillary pressures at low saturations that have been measured for Topopah Spring welded tuff could be due to a surface adsorption phenomenon (Marshall and Holmes, 1979). Thus, at low saturations, the "capillary condensation" may actually be condensation due to surface adsorption. It should be noted that condensation will not occur until the temperatures drop below the dew point on the WP itself because the WP walls are relatively smooth and, therefore, would not result in capillarity.

For $S < 10\%$, rewetting of the dried-out zone around the WP is dominated by vapor flow in fractures and capillary condensation. For $S > 10\%$, it was found in the long-term ECM calculations that rewetting is dominated by capillary imbibition. Therefore, for the purpose of the ECM calculations, rewetting of the host rock due to the bulk flow of liquid water begins to occur when $S_b = 10\%$ at the borehole wall, where S_b is the bulk saturation. For the reference case of 57 kW/acre with 10-yr-old waste in vertical boreholes, and for the 0.5- and 1.0-mm/yr cases, it takes about 1,000 yr for S_b to exceed 10% around the borehole wall (Table 8), while for the 0.1-mm/yr case, it takes 1400 yr.

These estimates are very conservative. For high APDs (i.e., hydrologic performance dominated by boiling effects), the ECM and boundary conditions employed in this study result in conservative estimates of the duration of boiling conditions and the spatial and temporal extent of rock dry-out for the following four reasons:

(1) Because it cannot handle nonequilibrium fracture-matrix flow, the ECM is not capable of adequately representing condensate shedding. Consequently, the ECM causes more condensate to be thermally perched above the dry-out zone than would occur had nonequilibrium fracture flow been adequately represented. Because

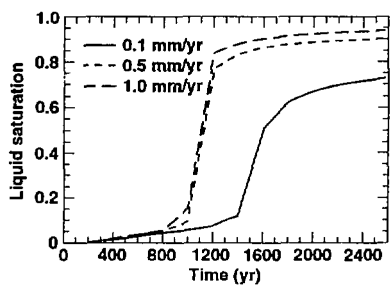

Figure 29. Liquid saturation at the WP borehole for steady-state recharge fluxes of 0.1, 0.5, and 1.0 mm/yr for 2600 yr. Calculation is for 8.6-yr-old spent fuel with an APD of 57 kW/acre.

the condensate shedding effect enhances the rate of rock dry-out, neglecting this effect results in the ECM underpredicting the extent of boiling and rock dry-out.

(2) Thermal perching of condensate also results in a more persistent gravity-driven heat pipe zone above the boiling zone. Because it can very efficiently transport heat, the heat pipe zone tends to more quickly dissipate thermal energy that would otherwise have been available for boiling and rock dry-out. Therefore, the tendency for the ECM to overpredict the extent of the heat pipe zone results in it underpredicting the extent of boiling.

(3) The water table is treated as a constant temperature, pressure, and saturation boundary. The assumption that the water table is a constant temperature boundary results in its acting as a heat sink, thereby resulting in its tending to limit the spatial and temporal extent of boiling conditions. Had the finite resistance to heat flow in the saturated zone been represented, boiling conditions would have persisted longer. The assumption that the water table is a fixed saturation boundary results in its being a huge source of water for re-wetting of the dry-out zone. Had the model been able to represent the water table as a movable boundary, the resulting depression in the water table surface would have allowed dry-out to persist to greater depth. Therefore, representing the water table as a fixed constant temperature, pressure, and saturation boundary tends to limit the spatial and temporal extent of boiling and rock dry-out effects.

(4) Hysteretic capillary pressure and relative permeability data are not available for the matrix. The currently available capillary pressure and relative permeability data for the matrix were obtained under drying conditions. Applying the characteristic curves determined by Peters and coworkers (1984) with the use of an oven psychrometer to imbibition calculations for Grouse Canyon densely welded tuff, Buscheck and Nitao (1987, 1988) found that a reasonable match between modeled and observed data was obtained if k_m was reduced by a factor of 40. This discrepancy could be attributed to uncertainty concerning k_m or to capillary hysteresis. Using data for the welded tuff TSw (Lin and Daily 1990), we obtained a reasonable match between modeled and observed imbibition data after applying a similar reduction in k_m. Therefore, the use of the drying curve data will significantly overpredict the rate at which the dry-out zone re-wets back to ambient saturation. Consequently, our calculations conservatively predict the duration of sub-ambient saturation conditions at the repository horizon. The estimates of dry-out and boiling condition durations discussed above are minimal durations. Therefore, saturation, and, thus, water movement into the emplacement openings will be minimal for at least 1,000 yr. Recent analyses indicate that this time may extend from 100,000 to 200,000 yr for 60-yr-old waste emplaced at 114 kW/acre (Fig. 27).

4.2.5 Humidity

The relative humidity at the surface of the WP can be estimated on the basis of the following assumptions. First, on the basis of the observation of Buscheck and Nitao (1991a) that the gas-phase pressures in the fractures remain very close to atmospheric during boiling, the assumption can be made that the gas-phase pressure is fixed at the initial atmospheric pressure at the repository horizon. Second, in order to be conservative, the assumption is made that the water-vapor pressure is equal to the gas-phase pressure. Based on these assumptions and the temperature calculations reported by O'Neal et al. (1984), the calculated range in relative humidity at the surface of the WP would be 3.9 to 35% for the central panels during the first 300 yr after emplacement (see Fig. 30). The relative humidities would be considerably different for temperature histories corresponding to other thermal loading scenarios. Note that although the relative humidity is less than 100%, the water mass fraction, x_{wg}, in the vicinity of the WP is 100% as long as boiling occurs. For certain thermal loading scenarios, the WP temperatures at the edge of the repository may never exceed the nominal boiling point (T_b = 96°C). For such locations, the relative humidity would remain close to 100% throughout the repository history.

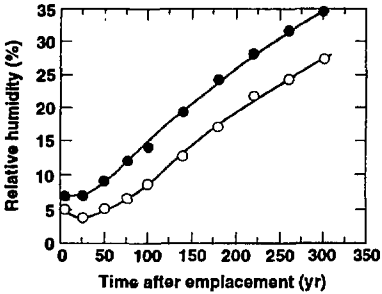

Figure 30. Maximum relative humidity predicted for the central boreholes at two locations, based on observations of Buscheck and Nitao (1991a) and calculations of O'Neal et al. (1984).

4.3 Radiation Effects of Waste Emplacement

Radiation effects are functions of the radiation dosage and the moisture/vapor composition within emplacement openings. Effects are not expected to extend beyond 1 to 2 cm into the rock mass. Radiation shielding or other design considerations can effectively eliminate the effects of radiation on the NFE.

The emplacement of a nuclear waste container may subject the immediate environment of the container to significant levels of gamma radiation on the basis of the current reference design. The interaction of gamma radiation with the near-environment of the WP is an important factor in assessing its overall performance (Van Konynenburg, 1986) because the radiolytic species generated can impact WP performance, and thus will have important implications for the selection of the container material (Reed et al., 1990; Reed and Van Konynenburg, 1991). However, technical concerns related to radiolysis can be substantially controlled through design options of both the repository and EBS. The most important aspects of the design are (1) shielding to reduce the gamma flux, (2) internal configuration of WP, (3) the free volume present in the near-WP environment, and (4) the overall repository temperature, which depends on the spacing and heat-loading of the WPs.

4.3.1 Self-Shielding and Internal Configuration

Self-shielding is usually accomplished by increasing the thickness of the container wall, but it could also include other design modifications such as placing filler material in the container. The idea of lowering the gamma dose rate by increasing the container thickness is not a new one. In the WP designed by the Swedish high-level waste (HLW) program that was approved for licensing, a 20-cm-thick container was proposed to attenuate the gamma flux and remove radiolysis as an issue. In the Basalt Waste Isolation Project, which was proposed for the HLW site formerly considered at Hanford, a thickness of 8.5 cm was proposed that was also defined by the need to attenuate the gamma-radiation flux outside the container.

The SCP reference container thickness proposed by the YMP was 1 to 3 cm, with 1 cm as the thickness that is most referenced. This thickness corresponds to an initial container surface dose rate as high as 0.1 Mrad/hr, corresponding to absorbed doses of 50,000 Mrad during the first 300 yr of repository history.

4.3.2 Free Volume Outside the Waste Container

In the unsaturated system, the radiolytic products are generated in the free volume or air gap between the container and the host rock in the reference borehole WP design. Minimization of the volume of this air gap would proportionally decrease the yield of radiolytic products and reduce the potential for radiolysis to affect container material degradation.

Although the design is not yet firm, any gap between the borehole wall and the emplaced container would probably not exceed 10 cm. This corresponds to a free volume of approximately 1200 L for each spent-fuel WP.

4.3.3 Temperature Impacts on Radiation Effects

From the perspective of corrosion in an irradiated air–water-vapor system, higher rather than lower temperatures are preferred. As long as temperatures of the WPs are higher than their surroundings, liquid water will not condense on the container surface, and this will reduce the likelihood of localized effects from radiolytic products.

The composition of the preemplacement gas phase has been well characterized as water-vapor-saturated air with up to 0.13 mole% carbon dioxide (Thorstenson et al., 1989). Within the total pressure constraint, the emplacement of high-level nuclear waste would affect the gas phase primarily by evaporating water. The range of conditions that are anticipated in the WP environment is (1) pure water vapor, (2) dry air, and (3) humid air (between the two extremes). The relative humidity, defined as the ratio of water vapor pressure to the equilibrium vapor pressure of water at that temperature, would be set by the availability of water and the temperature of the WP.

The radiation levels (for 10 to 20-yr-old spend fuel) at the container surface may be as high as 0.1 Mrad/hr for the thin wall WP design discussed in the SCP, but they will decrease rapidly with respect to repository-relevant times, with an effective half-life of approximately 30 yr. The total absorbed dose at the surface of the container will depend on the initial gamma flux present, which is a function of the design of the WP, the radionuclide content of the waste form (glass loading or burn up of the spent fuel), and the age of the waste form. To a first approximation, this value is proportional to the initial dose rate and is 5×10^{10} rad in the first 300 yr, for an initial dose rate of 0.1 Mrad/hr.

The expected environment for most of the containment period is an air–water-vapor mixture that would exist at temperatures from 27 to 250°C at a total pressure of 660 Torr. The key radiolytic products in this environment are (1) nitrogen fixation products: nitrogen acids, nitrogen oxides, and ammonia, (2) hydrogenous species: atomic and molecular hydrogen, and (3) oxygen-containing oxidizing species: oxy-radicals, ozone, and hydrogen peroxide. Argon, although it can affect homogeneous gas phase reactions by energy transfer, is stable to radiolytic decomposition. Carbon dioxide is slowly decomposed to oxygen and carbon monoxide and would undergo condensation reactions to generate higher molecular weight organic compounds.

The key step in the formation of nitrogen oxides is the radiation-induced breakdown of molecular nitrogen to atomic nitrogen. In dry-air and low-humidity systems, this then leads primarily to the direct formation of nitrogen dioxide and nitrous oxide along with trace concentrations of other oxides. Of the nitrogen oxides generated, nitrogen dioxide is the most important with respect to evaluating WP performance. In dry air it directly oxidizes the metal, and in humid air it is converted to nitric acid. This, depending on the relative humidity of the irradiated system, can be adsorbed onto the surface of the components of the WP, leading to potentially detrimental effects.

The reaction of the hydroxyl radical (OH) with nitrogen oxides to form nitrogen acids is thermodynamically favorable over the temperature range of interest to the YMP. Once formed, however, the acids are not thermodynamically stable with respect to the bulk components of the air–water-vapor mixture at elevated temperatures (above 120°C) and will undergo thermal decomposition. The kinetics of this process and the competitive process of nitrogen acid solvation in water films that are present have not been well characterized. The overall fate of the nitrogen acids at the elevated temperatures is therefore not well understood.

In the irradiated air–water-vapor system, the nitrogen oxides generated are rapidly converted to nitrogen acids by the OH radical generated from water vapor [G(OH) = 4.25 to as high as 8.2 molecules/100 eV] (Dixon 1970), where G is the radiation chemical yield. Nitric acid is the predominant product, since nitrogen dioxide is more stable in the irradiated system, and it persists at a higher concentration in the gas phase than does nitric oxide. In low-humidity systems, the yield of nitric acid is equal to the yield of nitrogen dioxide in the analogous dry-air system (same nitrogen/oxygen ratio). Figure 31, which is based on our work, shows the yield of nitrogen dioxide in the gas phase as a function of absorbed dose for dry and low-humidity air at 120°C.

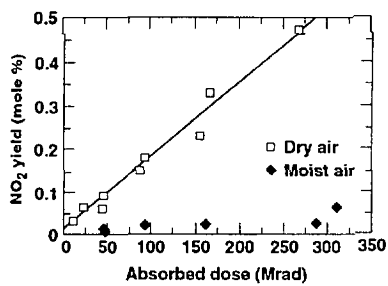

Figure 31. Yields of NO_2 in the gas phase for dry and low-humidity air at 120°C.

In high-humidity systems (e.g., water-vapor to air ratios greater than 0.1), the yield of nitrogen dioxide has not been well characterized. A nitrate yield of 1.9 was reported by Linacre and Marsh (1981) for mixed gamma and neutron radiation, and a yield of 2.5 was reported by Jones (1959) for high-dose-rate beta radiation. We have typically seen lower yields (0.5 to 1.5 molecules/100 eV) in the longer-term and lower-dose-rate gamma studies. The yield appears to depend on the ratio of water vapor to air of the system. Our initial results, which were obtained at 28 and 87°C, are shown in Fig. 32. For the purpose of modeling, yields in the range of 0.5 to 2.5 molecules/100 eV need to be considered.

The NFE temperatures will decrease as the waste decays. However, there is significant thermal inertia that will maintain elevated temperatures. Therefore, the potential for radiation effects will decrease significantly before the temperatures drop.

4.3.4 Nitrogen Oxides

For the temperatures and pressures relevant to the YMP, only nitrous oxide, nitric oxide, and nitrogen dioxide are important to consider. Figure 33 shows the concentrations of oxygen, nitrous oxide, and ammonia following irradiation of water vapor as a function of adsorbed dose.

4.4 Performance Implications

4.4.1 Hydrologic Equilibrium

Given the unsaturated conditions and the high matrix potential that is expected within TSw2, analyses indicate that fracture flow is not expected to occur over the large majority of the repository horizon. However, local conditions and episodic pulses of high infiltration heavy rainfall or the thermal perching of water driven off from the WP areas may allow fracture flow to occur on a spatially limited basis. Current design concepts for the EBS include a capillary barrier between the rock matrix and the WP itself. As long as this capillary barrier functions, there are no credible mechanisms for introducing water onto the WP itself, with the possible exception of condensation from vapor in the borehole or dripping water from a fracture. An appropriate design/configuration may develop a hydrothermal umbrella, which would mitigate

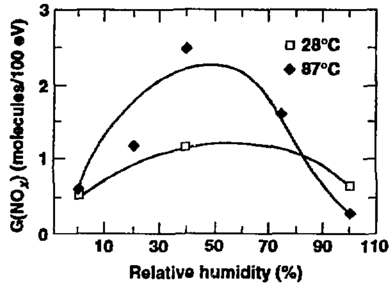

Figure 32. Yields of NO_x at 28 and 87°C.

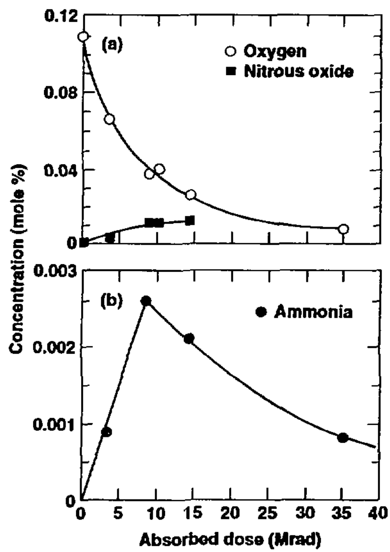

Figure 33. Concentrations of oxygen, nitrous oxide, and ammonia following irradiation of water-vapor-saturated 0.1% oxygen in a nitrogen mixture at 28 ± 2°C.

fracture flow. Therefore, the anticipated environment for the WP will be one which is essentially dry, with limited potential for localized fracture flow to occur. Because the fracture network consists of essentially vertical fractures, these fractures will allow for downward migration of any water within the fracture network. Depending upon the orientation of the waste emplacement, this water may flow harmlessly away from the region of the WPs or it could intersect the WP boreholes or drifts (Wilder, 1990).

The hydrologic behavior of the unsaturated zone depends on the balance between fracture and matrix dominated flow. Due to small matrix permeability, matrix-dominated flow will not result in significant vertical transport of radionuclides. Fracture-dominated flow is the only credible means for liquid water contact with the WP. Preliminary field evidence indicates the potential for fracture-dominated flow penetrating to considerable depths. Analyses also indicate that, because the flow in fractures and matrix blocks is not in capillary equilibrium during episodic infiltration events, episodic fracture flow may be possible even under unsaturated conditions.

Fracture flow is also a function of fracture network discontinuities, which are not well characterized at this time, dispersion of liquid flow in fracture networks, which is also a function of the fracture networks and is not well characterized at this time, and fracture-matrix interactions. Hydrological performance assessment will be very sensitive to the nature of vertically connected fracture networks in the low permeability welded and zeolitized nonwelded units. The high permeability of the vitric nonwelded tuffs may result in very substantial lateral matrix flow. The interaction of this lateral flow with vertically contiguous faults is a critical hydrological performance issue. Therefore, assessing the hydrological performance of the repository system, particularly the preliminary assessments required to demonstrate site suitability, will need to focus on whether (or how) fracture networks in the welded units facilitate fracture-dominated flow.

As has been discussed, for all but the lowest-APD disposal scenarios, waste-generated heat will cause moisture to be driven out of the repository host rock. The elevated temperatures will maintain dry-steam conditions for hundreds to thousands of years, depending on the design options chosen. Likewise, once water is removed from the system, it takes a long time for resaturation of the rock mass. Both of these processes will minimize, if not eliminate, any water contact with the WPs.

The environmental conditions change with time, and the natural heterogeniety in those conditions also varies with time. This is depicted conceptually for the saturation conditions in Fig. 10. The initial saturation conditions are expected to be normally distributed around a mean of 65% with a standard deviation of ±19%. As waste is emplaced, the saturation is expected to approach 0% with a much tighter distribution around this mean. This is shown in the conceptual drawing (Fig. 10) as the emplacement case, where the conceptualization of postemplacement saturation distribution is very much skewed towards zero values to reflect the very dry conditions that result from heating of the rock mass. The distribution shows a spike somewhat above zero to account for the possibility of some small percentage of the WPs, particularly those in the outer regions of the repository, to have some moisture in the near field. However, based on the temperature calculations referred to above, it is unlikely that the NFE associated with any of the WPs will have moisture above a few percent, and the conceptualization is likely overly conservative.

For the reference case, resaturation is shown on the time history conceptualization (see Fig. 10) assuming that at 1,000 yr, moisture conditions for the coldest packages will tend towards ambient, but for most of the repository area, saturations will be in the 10% range, as noted in Sec. 4.2.4. Therefore, the saturation for the ensemble of all containers will have a more broadly spread distribution, with a mean only slightly increased above the early postemplacement values. Because the temperature history is a function of design and operations of the repository (which are yet to be determined), no specific analyses have been performed to determine how rapidly this cooling will take place. Therefore, the rate of change in the saturation distribution has been determined for a range of design options. A design specific analysis will have to be made later.

It has been demonstrated during field studies that the rewetting takes much longer than the drying cycle (Ramirez et al., 1991). The time for rewetting is dependent on thermal loading and thus volume of rock dried out, and also on the temperature decline and capillary rewetting diffusivity of the rock [see Vol. II, Sec. 1.0, and Buscheck and Nitao (1992)]. It has also been demonstrated that rewetting from vapor phase capillary condensation is only effective up to 10 to 20% saturation. Therefore, after liquid water has been driven off, the saturation of the rock will not be elevated to above ~20% until liquid water is able to return to the NFE. Given the long period of elevated borehole wall temperatures (as much as 10,000 yr above or near to the boiling point at higher APDs with older fuel), it is likely that the NFE will remain dryer than ambient well beyond 1,000 yr (shown conceptually in Fig. 10), and possibly for much longer than 10,000 yr. Given the temperature distribution shown, it is very likely that the NFE will continue to be essentially dry for at least 1,000 yr for the reference case and possibly for over 100,000 yr for 114-kW/acre 60-yr-old waste.

Following total dissipation of the thermal pulse, and after sufficient time has elapsed to allow moisture redistribution to occur over the entire altered zone, a hydrologic equilibrium condition will be reached. This distribution will match the original ambient distribution only if there is sufficient moisture in the system to replace that which had been removed by the construction and emplacement processes or that drained away from condensation zones. It is assumed that it will take considerably longer than 1,000 yr for the moisture to be replaced. The distribution is shown conceptually in Fig. 10 assuming that 10,000 yr after emplacement, all temperature and hydrologic perturbations will have dissipated. However, as mentioned, this may be overly conservative, even for the reference case.

Fracture-matrix interactions are functions of the fracture and matrix properties. However, dry-out due to thermal loading can have an overriding influence on the matrix properties and fracture-dominated flow. The thermal loading is very dependent on design and operational details. Therefore this section will give characterization information for a series of possible designs.

4.4.2 WP/Hydrologic Interactions

An important environmental consideration is the state of any water or moisture contacting the WPs. As already discussed, liquid water is not expected, particularly if higher APDs are used. The air/vapor present in the pore space and therefore available to contact the WP is expected to be moist air (essentially 100% relative humidity) during pre-emplacement times. After waste emplacement heating occurs, water in the pores will be either evaporated at an increased rate for temperatures below the boiling point or turned to vapor or steam if temperatures are above boiling. For below boiling temperatures, the emplacement openings would be expected to be filled with humid air. In the above boiling case (particularly once dry-out occurred and temperatures increased above the BP), the environment would be dominated by dry steam (100% water vapor—no liquid water).

One potential benefit of older waste is that spacing can be decreased to obtain the same emplacement APD, which will result in even greater elevation of temperatures overall without the significant peak and subsequent decay. This results in higher long-term temperatures, as shown in Fig. 34. Therefore, with proper balancing of age and APD, the temperatures can be maintained above boiling for extremely long periods of time. An additional benefit is that repository area can be decreased, as shown in Table 12. This may appear to be only an economic or operational benefit. However, a smaller area requirement would give greater flexibility to respond to the geologic/hydrologic variability in nature. For example, a smaller repository could be kept further from major faults and could be placed under the thickest and most consistent portions of the nonwelded units that would stop infiltration or over the portions of the areally discontinuous sorptive units.

The percentage or amount of water shedding can be controlled by repository design options such as increased drift spacing, loading sequencing, and age of waste. As seen in Fig. 35, the majority of the condensate, regardless of waste age, is generated

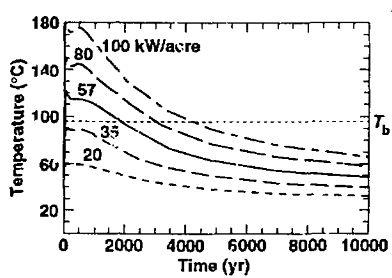

Figure 34. Drift-wall temperature for drift emplacement of 30-yr-old spent fuel and zero recharge flux. Dry-steam boiling conditions persist at the WP environment for thousands of years for high APDs.

Table 12. Repository area requirements as a function of areal power density (APD) and spent-fuel age (shown as the ratio of the area requirement to the SCP[a] reference area).

	20 kW/acre	36 kW/acre	57 kW/acre	80 kW/acre	100 kW/acre	114 kW/acre
10-yr-old fuel	2.85	1.57	1.00	0.71	0.57	0.50
30-yr-old fuel	1.81	1.00	0.64	0.45	0.36	0.32
60-yr-old fuel	1.14	0.63	0.40	0.29	0.23	0.20
100-yr-old fuel	0.73	0.40	0.25	0.18	0.15	0.12

[a]MacDougall et al. (1987). SCP reference area is 1,380 acres.

during the first 100 yr after emplacement, so that proper design can remove a significant portion of the water originally in the pores.

Since matric potential is a function of the degree of saturation, during the period when the near field is very dry there is little possibility for pore water to contact the WPs. Even given the conservative reference case and high flux conditions of 1.0 mm/yr, analyses indicate that at no time within the 2600-yr time span is water able to enter the borehole (Nitao, 1988). Since corrosion is a function of contact with water, this would mean that the containers would be anticipated to have at least a 1,000-yr lifetime and, as discussed previously, a much longer time until aqueous contact with WPs is likely. In addition, fracture flow is influenced by the imbibition of water into the matrix. The volume of rock dried out is very large (depending on the APD and thermal characteristics

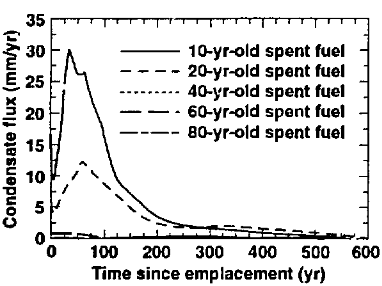

Figure 35. Net condensate generation flux averaged over the entire repository for 15-ft center-to-center spacing of 10, 20, 40, 60, and 80-yr-old PWR spent fuel.

of the disposed waste), and thus imbibition capacity is very large. Thus the potential for fracture flow to impact the WPs is unlikely, and imbibition would inhibit the movement of any radionuclides that might escape the WPs.

Current estimates are that pore water will not travel through the pores of TSw2 (porous media flow) until somewhere around 80% saturation is reached because the relative hydraulic conductivity remains low until nearly 80–90% saturation (Buscheck and Nitao, 1988). Also, water will not flow from the pores in the matrix to enter openings with diameters larger than the pores themselves since the capillary forces are an inverse function of the pore or opening diameter. This is the basis of one WP conceptual design option as discussed in the SCP, wherein there is a capillary barrier between the WP and the borehole wall so that no pore water should contact WPs.

As long as conditions remain unsaturated and the capillary barrier remains (no WP contact with borehole walls or sloughing of rock into boreholes), there is no mechanism to allow liquid water from the pores to contact the WPs. Thus, fracture flow is the only credible mechanism to bring liquid water into contact with the WPs. Fracture flow, under capillary equilibrium between matrix and fractures, is not expected unless the matrix adjoining the fracture is nearly saturated (about 95%), depending on the fracture characteristics. Fracture flow can occur either under conditions where the matrix becomes nearly saturated or for persistent ponding conditions above relatively large apertures, but for the strata being evaluated as a possible repository horizon there is minimal possibility of static ponded conditions and thus continual fracture-dominated flow even in major fault systems (Nitao, 1991). As stated earlier, it is possible for fracture flow to occur in response to infiltration pulses or ponding that exceed the rate of imbibition, and this fracture flow can occur to considerable depths (Nitao and Buscheck, 1989). This nonequilibrium episodic flow must be considered in design.

Flow through the fractures only continues as long as the source continues to "pond" water at the fracture entrance. Once the source of water is taken away, any fracture flow ceases. This has implications for the potential for water to contact WPs. If there is fracture flow from a heavy recharge event, that flow can occur only as long as the precipitation or surface ponding continues. Theoretically, the maximum flow that can occur through a 100-μm fracture at the entrance to the fracture is 100 L/day/m of fracture opening length if the fracture is fully saturated with plane flow (no channeling) that obeys the cubic law.

Unless ponded flow conditions at the infiltration source allow for the storage of very large volumes, the ponded source of infiltration flow may only persist for relatively short periods of time. A possible exception (of a limited ponded volume) is if the high permeability and porosity of the nonwelded vitric tuff or PTn results in the development of a perched saturated zone which then acts as a ponded infiltration source (perhaps for a significant duration). With the exception of the impact of this potentially large "ponded" storage volume, most fracture flow reaching the WP borehole may be of limited duration. Moreover, the actual flow rates attributed to even relatively large aperture fractures are relatively small. Therefore, the quantity of water contacting the WP may be limited in both quantity and duration. Whether or not liquid water will contact a WP will depend on the answers to two additional key questions: (1) whether the fractures intersecting the WP borehole are part of a fracture pathway that is hydraulically connected to an overlying source of water, and (2) the minimum effective hydraulic aperture of this connected pathway.

On the basis of the work of Nitao and Buscheck (1989) and Buscheck and Nitao (1988a, 1991a,b), if any pulse of fracture flow is to be able to reach the WP borehole, it will do so over a relatively short time frame. The time it will take the liquid front to travel from the infiltration source (e.g., alluvial deposits in washes) to the WP could be from days to months. The hydrological performance and site suitability analyses of these events must account for the transient, spatially heterogeneous behavior of nonequilibrium fracture network-matrix flow.

The cases in which water may be able to flow through fractures are likely to be exceptional rather than typical. It has been shown that even for saturated sites, the natural heterogeneity is such that most of the water flow is from a small percentage of the rock mass. While this is true even of soils, it is particularly true for fracture-dominated flow. Studies at the Stripa site (Neretneiks, 1985), which is located in fractured granite below the water table, indicate that flow through fractures is very heterogeneous, with a small percentage of the area being responsible for the majority of the flow. These observations are consistent with observations at other sites. LLNL has extended work in the petroleum fields, combined with information from Stripa, to develop an approach which allows the heterogeneity to be accounted for. This work is preliminary and applicable to Yucca Mountain conceptually; however, we feel that the approach is valid even if the actual numbers may be wrong. Figure 36 shows an assessment that was made on the basis of professional judgement as to what might be expected at Yucca Mountain for the reference emplacement case of 57 kW/acre and 10-yr-old fuel. As can be seen, it is anticipated that only a very small percentage of the repository would have water flowing in fractures. Further, it is possible that the features that would carry water can be identified by careful field inspection so that these areas could be avoided. On the basis of this analysis, as well as the ones discussed in the sections above regarding water removal and dry out, it is felt that the vast majority of WPs will be in

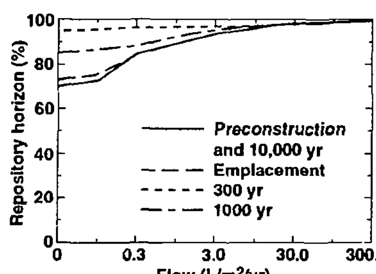

Figure 36. Cumulative flow volumes for the reference case. Suggested design water flow values based on 95% of repository area conditions would be 0 $L/m^2/yr$ for 300 yr, and less than 5 $L/m^2/yr$ for preconstruction or 10,000 yr cases.

a dry environment for their entire lifetimes, and that even those which may be in an area where there is fracture flow will not have water contact until several hundred or thousands of years after emplacement, depending on whether low or high APDs are employed.

Thus it can be concluded that except for extreme, short-duration, episodic events, nonequilibrium fracture-dominated flow is unlikely. As previously explained, fracture flow will only occur as long as there is a source of ponding, which causes fracture flow to dominate over imbibition. Fracture flow will occur through the interconnecting fracture network, and since many fractures are discontinuous, the most likely pathways for fracture flow are the more major through-going fractures, e.g., fault zones or major fracture systems. This being the case, if there is sufficient water to cause fracture-dominated flow to reach the repository horizon, it might continue to flow in the through-going fractures rather harmlessly past the repository horizon. Once the source of water was depleted, fracture-dominated flow would cease and the water remaining in the fractures would be imbibed into the matrix, where it would essentially be immobilized and not able to contact the WPs.

4.4.3 Condensate Drainage

The most likely source of water to contact the WPs would be water from the dried-out zone condensing above the WP and then flowing through fractures into the WP boreholes (Wilder, 1990). The potential for this to take place is very much dependent on ultimate repository layout, etc. One of the design factors under consideration is the optimizing of thermal loading, which is a natural consequence of any waste emplacement, so that the condensate is shed to the pillar areas and will not build up in the area above the WPs. For a significant portion of the dry-out period, there will be preferential drainage away from the WP emplacement holes and drifts (Wilder, 1990). Prototype experiments in G-Tunnel have shown that a considerable portion of the condensate drains down fractures, so that large volumes of condensate cannot collect above the WPs. The concept of drainage away from the rock mass immediately above the emplaced waste is shown in Fig. 37, and with appropriate spacing, most of the condensate would be shed to the pillar area. This shedding would be active until the temperatures were raised over the repository area sufficiently for the boiling point isotherms to coalesce between emplacement

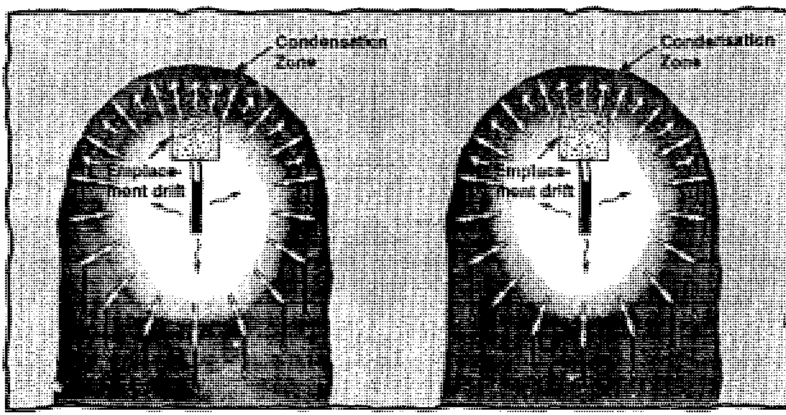

Figure 37. A "hydrothermal umbrella" is established along each of the emplacement drifts because of condensate being shed off the sides of the boiling zone.

drifts. At that point the condensate might remain in a condition of thermal perching until the temperatures began to drop. However, it is important to note that even if condensate is perched, two processes will mitigate any contact with the WPs. The first is the imbibition into the matrix. Since the thermal perching may last for several thousand years, there is ample time for the condensate to be imbibed into the matrix, where it would not be available for flow in the fractures to the area of the waste. The second is the fact that the cooling will follow the same general pattern as the heating, so that the pillar areas will cool below the boiling point prior to the emplacement opening surfaces. This will then allow for drainage of any condensate that was not imbibed.

Even if the 20 m^3 of water [the calculated maximum amount of water that could possibly be generated per m^2 of repository area (Wilder, 1990)] were to collect, it would be unlikely that all of this water would be able to flow into contact with WPs. As the temperatures started to drop, water would flow preferentially down fractures in the midpillar regions where the boiling point isotherm retreat would be greatest. The boiling point isotherm retreat is very slow, so that by the time the temperature no longer shielded the WPs, condensate drainage would be negligible. Since it would take hundreds to thousands of years for the temperatures to drop below boiling in the very near field, there would be sufficient time for any water that did not drain through pillar areas to be imbibed into the matrix that had been dried out. If the entire volume of water were able to drain unrestricted down the fractures, and assuming 20 fractures/m^3 of rock, it would only take 10 days to drain the water out of the condensation zone, at which time the flow would stop and be imbibed. Thus, no water is expected to enter the emplacement holes or drifts, and if it did, it could be drained rapidly away. This assumes no backfill; however, backfill may act to inhibit water entry (depending on backfill design).

Calculations for different-age waste and various APDs indicate that the time at which the rock mass remains above the boiling point may be extended to thousands or even tens of thousands of years depending on the designs chosen. The period during which the rock remains dry is much longer than the period of elevated temperatures. Conservative analyses that do not consider condensate drainage indicate that the system will not return to ambient conditions for 100,000 to 200,000 yr if high APDs are used. Considering the effects of condensate drainage should make the time for ambient conditions to return even longer. Furthermore, appropriate repository pathways for drainage of water above the repository level will remain for extended periods of time, which would facilitate the drainage of water to positions below the waste emplacement level, thus removing it from potential contact with the waste (Buscheck and Nitao, 1992).

4.4.4 Aqueous Flow of Potential Radionuclide Transport

Given the extremely small matrix permeability throughout most of the unsaturated zone, matrix-dominated flow is too slow to be of concern for radionuclide transport. Moreover, the high suction potential of the matrix will result in the WP borehole being drained of water under the low recharge fluxes associated with matrix-dominated flow. As long as the rock around the WP remains partially saturated and the capillary barrier is intact (no WP contact with the borehole walls or sloughing of rock into the boreholes), there is no mechanism other than fracture flow to allow water to contact the WPs. It is also unlikely that low recharge fluxes associated with matrix-dominated flow will be sufficient to result in a seepage face along the ceiling of the emplacement drift. Fracture-dominated flow, particularly as it may occur along networks of vertically connected fractures, provides the most likely means for water to contact the WPs, thereby accelerating their failure and transporting radionuclides to the water table. Fracture-dominated flow only occurs when a sustained source of water at the entrance of a fracture pathway results in fluxes sufficient to overwhelm the capacity of the matrix to imbibe that flow. Such large, sustained fracture fluxes cause flow in the fracture to be out of capillary pressure equilibrium with flow in the matrix, resulting in the wetting front in the fracture advancing much faster than the wetting front in the matrix.

The amount of water that could contact the WPs, even under the extreme conditions sufficient to allow fracture flow to extend to the repository horizon depths, would be limited both in quantity and contact time. Since any flow that takes place will be within the fractures, transport will occur only when there is sufficient source to cause fracture flow. As already mentioned, these conditions will be episodic, since the mountain is not saturated and recharge occurs sporadically.

Furthermore, if water were able to contact waste forms and leach radionuclides, it would be imbibed into the matrix as soon as the source of the pulse was removed. This would imply that radionuclides would not leave the altered zone for many thousands of years. Even at ambient conditions, matrix flow does not occur and fracture flow only occurs in pulses, which are ultimately imbibed into the matrix along with any dissolved radionuclides. Heavy recharge events along continuous fractures are a potential source of ponding with sufficient duration and volume of water to cause flow to reach the water table. These events would be the heavy rainfall events that in this arid environment typically last for a few hours or days at most. The overlying units act as barriers to infiltration of this water except in major through-going fracture systems, which are typically faults, not the jointing that is ubiquitous. Thus, it is unlikely that water from recharge will be able to flow through the repository area, contact waste, and then flow on to the water table.

A second source of ponding would be saturation of the overlying nonwelded tuff units, which would then expose the ubiquitous joints to ponded conditions. However, down-dip flow would occur in these units, so that saturation of these units over extensive areas is unlikely. If saturation of perching in these units did occur, it would dissipate rapidly with fracture-dominated flow in the lower units.

A final source of water that could be ponded is condensate water. If condensate is not able to drain because of the rock temperatures exceeding boiling, a thermal perching may result. While analyses indicate that these conditions are not likely, then cannot be entirely ruled out. Clearly, fracture-dominated flow of this water cannot occur until temperatures drop below boiling (otherwise there could be no thermal perching). Since temperatures in pillars and areas away from waste will drop faster than in areas near the waste, fractures in the pillar areas will drain any thermally perched condensate before it can drain through fractures that could bring water in contact with waste.

Analyses have been performed to determine wh[illegible] radionuclides transported by a pulse that is [illegible]ipated will then be available to be picked up in the next pulse and carried along. It was found that as long as the wetting diffusivity is significantly greater than molecular diffusivity (the expected condition at Yucca Mountain), and unless pulses were closely spaced in time, water and any dissolved radionuclides that had resulted from the first rapid infiltration pulse would be imbibed such that the next but larger pulse would not see the previous pulse. Therefore, fracture flow is not directly additive in that successive pulses cannot push the majority of the previous pulses further down the fracture. It is only when the duration as well as quantity of infiltration is much greater than expected for Yucca Mountain that water can flow along fractures for the significant distances necessary to contact the WPs. Analyses indicate that standing water that remains for 48 hours at the entrance of a fracture may migrate as much as 100 m in a 100-µm fracture before the pulse is dissipated (Buscheck and Nitao, 1988; Nitao and Buscheck, 1989).

These conclusions do not apply to radionuclides transported as colloids. If there are any radionuclides carried as colloids, they may filter out on the walls of fractures but would not be moved further unless a more significant pulse occurred to pluck the colloidal-sized materials off of the fracture surfaces. Even in this case, once the colloids are dried, these materials may form fracture coatings that are not readily picked up by subsequent water pulses. Furthermore, between fracture flow pulses, radionuclides may diffuse into the matrix. Thus it is not known at this time whether these radionuclides may be carried deeper by succeeding pulses.

4.4.5 Diffusion-Controlled Radionuclide Transport

If fracture-dominated flow is able to reach emplacement openings in TSw2, lateral penetration of the wetting zone into the matrix will occur (Buscheck and Nitao, 1991a,b). This penetration will be on the order of centimeters (Table 13). Therefore, even under these unlikely occurrences, the associated changes in the matrix saturation should be relatively minor. The primary impact of matrix saturation on diffusion-controlled releases of radionuclides is to increase the apparent molecular diffusivity with saturation. Therefore, fracture flow may not significantly enhance diffusion-controlled release modes.

If fracture flow cannot reach a WP, then radionuclide releases will be limited diffusion-controlled release modes. These release modes will be facilitated by (1) the presence of a borehole backfill, or (2) sloughing of the WP borehole wall if a borehole backfill is not used. Although the rock at the repository level is unsaturated, a sufficient amount of pore water could form a contiguous diffusion path from the WP to (and through) the near-field rock matrix. The primary impact of

Table 13. Maximum lateral spread (m) of the wetting zone in the matrix.

	Fracture aperture (µm)					
	10	50	100	200	400	1000
TSw2	4.15	3.54×10^{-2}	6.26×10^{-3}	2.32×10^{-3}	1.08×10^{-3}	4.48×10^{-4}
TSw3	0.90	5.47×10^{-3}	9.68×10^{-4}	3.59×10^{-4}	1.61×10^{-4}	6.92×10^{-5}
CHnv	5.92×10^{3}	47.3	6.08	0.80	0.11	6.74×10^{-3}
CHnz	68.7	0.55	6.97×10^{-3}	9.27×10^{-3}	2.06×10^{-3}	1.01×10^{-3}
PPw	7.0×10^{2}	5.60	0.71	9.0×10^{-2}	1.28×10^{-2}	5.30×10^{-3}

matrix saturation on diffusion-controlled releases of radionuclides is its effect on the apparent molecular diffusivity (a secondary effect being its impact on the storativity of the diffusive system). Because the tortuosity of the connected liquid-filled pores decreases with saturation, the apparent molecular diffusivity increases with saturation.

For situations in which fracture flow does not come into direct contact with the WP, molecular diffusion through the matrix can provide a "bridge" between a failed WP and water flowing down a fracture. A very slowly growing region of contaminated matrix will develop as radionuclides diffuse through the backfill and out into the matrix of the host rock. Any flowing fracture intersecting this growing plume of contamination within the matrix has the potential of entraining radionuclides from the matrix immediately adjacent to the wetted region of the fracture and transporting them down the fracture. Fracture-to-matrix transport of radionuclides is driven by diffusion from regions of high concentration in the contaminated matrix to lower concentration in the water flowing in the fracture. However, as water is flowing down the fracture, it is also being continually imbibed by the adjacent matrix. Depending on the relative magnitude of the molecular diffusivity and capillary wetting diffusivity of the matrix, the diffusive flux of radionuclides from matrix to fracture may be overwhelmed by the advective capillary flux of water out of the fracture, thereby substantially limiting the mass of radionuclides that may be entrained by flow in the fracture.

References

Arulmoli, K., and C. M. St. John (1987), *Analysis of Horizontal Waste Emplacement Boreholes of a Nuclear Waste Repository in Tuff*, Sandia National Laboratories, Albuquerque, NM, SAND86-7133. (NNA.870601.0060)

Bauer, S. J., J. F. Holland, and D. K. Parrish (1985), "Implications About In Situ Stress at Yucca Mountain," *Proceedings of the 26th U.S. Symposium on Rock Mechanics*, E. Ashworth, Ed. (A. A. Balkema, Rotterdam, The Netherlands), pp. 1113–1120. (NNA.890518.0147)

Buscheck, T. A. (1990), personal communication.

Buscheck, T. A., and J. J. Nitao (1988), Estimates of the Width of the Wetting Zone Along a Fracture Subjected to an Episodic Infiltration Event in Variably Saturated, Densely Welded Tuff, Lawrence Livermore National Laboratory, Livermore, CA, UCID-21579.. (NNA.891018.0047)

Buscheck, T. A., and J. J. Nitao (1991a), Modeling Hydrothermal Flow in Variably Saturated, Fractured, Welded Tuff During the Prototype Engineered Barrier System Field Test of the Yucca Mountain Project, Lawrence Livermore National Laboratory, Livermore, CA, UCRL-ID-106521. (NNA.911212.0238)

Buscheck, T. A., J. J. Nitao, and D. A. Chesnut (1991), *The Impact of Episodic Nonequilibrium Fracture Matrix Flow on Repository Performance*, Lawrence Livermore National Laboratory, Livermore, CA, UCRL-JC-106759.

Buscheck, T. A., and J. J. Nitao (1992), *The Impact of Thermal Loading on Repository Performance at Yucca Mountain*, Lawrence Livermore National Laboratory, Livermore, CA, UCRL-JC-109232.

Buscheck, T. A., J. J. Nitao, and D. A. Chesnut (1991b), "The Impact of Episodic Nonequilibrium Fracture-Matrix Flow on Geological Repository Performance," *Proc. of the ANS Topical Mtg. on Nuclear Waste Packaging, Focus '91*, Las Vegas, NV, Sept. 30–Oct. 2, 1991; Lawrence Livermore National Laboratory, Livermore, CA, UCRL-JC-106759. (NNA.911231.0023)

Buscheck, T. A., and J. J. Nitao (1992), *The Impact of Thermal Loading on Repository Performance at Yucca Mountain*, Lawrence Livermore National Laboratory, Livermore, CA, UCRL-JC-109232. (NNA.920408.0008)

Carlos, B. (1985), Minerals in Fractures of the Unsaturated Zone from Drill Core USW-G4, Yucca Mountain, Nye County, Nevada, Los Alamos National Laboratory, Los Alamos, NM, LA-10415-MS. (NNA.920506.0037)

Carlos, B. (1989), Fracture-Coating Minerals in the Topopah Spring Member and Upper Tuff of Calico Hills from Drill Hole J-13, Los Alamos National Laboratory, Los Alamos, NM, LA-11504-MS. (NNA.881220.0001)

Daily, W., W. Lin, and T. Buscheck (1987), "Hydrological Properties of Topopah Spring Tuff—Laboratory Measurements," *J. Geophys. Res.* 92(B8), 7854–7864. (NNA.900123.0064)

Dixon, R. S. (1970), "Dissociation of Water Vapor by Photolytic, Radiolytic and Electron Impact Methods," *Rad. Res. Rev.* 2, 237. (Readily available)

DOE (U.S. Department of Energy) (1988), *Site Characterization Plan, Yucca Mountain Site, Nevada Research and Development Area, Nevada*, Office of Civilian Radioactive Waste Management, Washington, DC, DOE/RW-0199. (HQO.881201.0002)

DOE (U.S. Department of Energy) (1990), *Yucca Mountain Project Reference Information Base*, Version 4, Yucca Mountain Site Characterization Project Office, Las Vegas, NV, YMP/CC-0002. (NNA 890330.0077)

Dudley, Jr., W. W., W. E. Wildon, and D. T. Hoxie (1990), "Hydrologic Framework of the Yucca Mountain Area, Nevada," *Proc. Int. Symp. on Unique Underground Structures*, (Colorado School of Mines Press, Colorado). (NNA.900403.0205)

Durham, W. B., J. M. Beiriger, M. Axelrod, and S. Trettenaro (1986), "The Effect of Gamma Radiation on the Strength and Elasticity of Climax Stock and Westerly Granites," *Nuclear and Chemical Waste Management* 6, 159–168. (NNA.900109.0001)

Ehgartner, B. L., and R. C. Kalinski (1988), *A Synopsis of Analyses (1981–1987) Performed to Assess the Stability of Underground Excavations at Yucca Mountain*, Sandia National Laboratories, Albuquerque, NM, SAND88-2294. (NNA.881202.0203)

Flint, A. (1991), personal communication with Alan Flint from the U.S. Geological Survey on the topic of "Annual Precipitation Measurements at Yucca Mountain." (N/A)

Glassley, W. E. (1986), *Reference Waste Package Environment Report*, Lawrence Livermore National Laboratory, Livermore, CA, UCRL-53726. (NNA.920506.0035)

Harrison-Giesler, D. J., R. P. Morissett, and L. J. Jardine (1991), *Yucca Mountain Site Characterization Project Waste Package Plan*, YMP-90/62, Lawrence Livermore National Laboratory, Livermore, CA, UCRL-JC-106161. (NNA.920529.0030)

Jones, A. R. (1959), "Radiation-Induced Reactions in the N_2-O_2-H_2O System," *Rad. Res.* **10**, 655. (Readily available)

Kana, D. D., B. H. G. Brady, B. W. Vanzant, and P. K. Nair (1989), *Critical Assessment of Seismic and Geomechanics Literature Related to a High-Level Nuclear Waste Underground Repository*, Nuclear Regulatory Commission, Center for Nuclear Waste Regulatory Analyses, San Antonio, TX. (HQX.910624.0018)

Kemeny, J., and N. Cook (1990), "Rock Mechanics and Crustal Stress," *Demonstration of a Risk-Based Approach to High-Level Waste Repository Evaluation*, R. K. McGuire, Ed., Electric Power Research Institute, Palo Alto, CA, EPRI NP-7057. (NNA.910813.0004)

Klavetter, E. A., and R. R. Peters (1986), *Estimation of Hydrologic Properties of an Unsaturated, Fractured Rock Mass*, Sandia National Laboratories, Albuquerque, NM, SAND84-2642. (NNA.870317.0738)

Klavetter, E. A., and R. R. Peters (1987), *An Evaluation of the Use of Mercury Porosimetry in Calculating Hydrologic Properties of Tuffs from Yucca Mountain, Nevada*, Sandia National Laboratories, Albuquerque, NM, SAND86-0286-UC-70.. (NNA.890327.0056)

Klavetter, E. A., and R. R. Peters (1988), "A Continuum Model for Water Movement in an Unsaturated Fracture Rock Mass," *Water Resources Research* **24**, 416–430. (NNA.900719.0082)

Knauss, K. G. (1987), "Zeolitization of Glassy Topopah Spring Tuff under Hydrothermal Conditions," *Mat. Res. Soc. Symp. Proc.*, vol. 84, pp. 737–745. (NNA.920302.0050)

Knauss, K. G., and D. W. Peifer (1986), Reaction of Vitric Topopah Spring Tuff and J-13 Groundwater under Hydrothermal Conditions Using Dickson-Type, Gold-Bag Rocking Autoclaves, Lawrence Livermore National Laboratory, Livermore, CA, UCRL-53795. (NNA.891102.0117)

Knauss, K. G., J. M. Delany, W. J. Beiriger, and D. W. Peifer (1986), "Hydrothermal Interaction of Topopah Spring Tuff with J-13 Water as a Function of Temperature," *Mat. Res. Soc. Symp. Proc.*, vol. 44, pp. 539–546.. (NNA.870407.0364)

Lin, W. (1990), *Variation of Permeability with Temperature in Fractured Topopah Spring Tuff Samples*, Lawrence Livermore National Laboratory, Livermore, CA, UCRL-JC-104765. (NNA.910523.0105)

Lin, W., and W. D. Daily (1989), "Laboratory Study of Fracture Healing in Topopah Spring Tuff—Implications for Near Field Hydrology," *Proc. of the ANS Topical Mtg. on Nuclear Waste Isolation in an Unsaturated Zone, Focus '89* (American Nuclear Society, La Grange Park, IL), p. 443. (Readily available)

Linacre, J. K., and W. R. Marsh (1981), "The Radiation Chemistry of Heterogeneous and Homogeneous Nitrogen and Water Systems," Chemistry Division AERE Harwell, Didcot, Berkshire, England, AERE-R-10027. (NNA.920302.0066)

MacDougall, H. R., L. W. Scully, and J. R Tillerson, (Compilers) (1987), *Site Characterization Plan Conceptual Design Report*, Sandia National Laboratories, Albuquerque, NM, SAND84-2641. (NNI.880902.0014)

MacIntyre, A. T., D. Chesnut, and W. J. O'Connell (1990), Disruptive Scenario Aspects Important to Source Term Performance," Lawrence Livermore National Laboratory, Livermore, CA, UCRL-JC-104769. (Abstract)

Marshall, T. J., and J. W. Holmes (1979), *Soil Physics* (Cambridge University Press, England). (NNA.89121.0026)

Montazar, P., and W. E. Wilson (1984), *Conceptual Hydrologic Model of Flow in the Unsaturated Zone, Yucca Mountain, Nevada*, U. S. Geological Survey, Lakewood, CO, WRIR-84-4345. (NNA.890327.0051)

Moore, D. E., C. Morrow, and J. Byerlee (1986), "High-Temperature Permeability and Groundwater Chemistry of Some Nevada Test Site Tuffs," *J. Geophys. Res.* 91(B2), 2163–2171. (Readily available)

Neretneiks, I. (1985), "Transport in Fractured Rocks," *Proceedings, Memoires of the 17th International Congress of IAH, Tucson, AZ, Vol. XVII*, pp. 301–318. (NNA.900720.0078)

Nimick, F. G., and B. M. Schwartz (1987), *Bulk, Thermal, and Mechanical Properties of the Topopah Spring Member of the Paintbrush Tuff, Yucca Mountain, Nevada*, Sandia National Laboratories, Albuquerque, NM, SAND85-0762. (NNA.870723.0015)

Nitao, J. J. (1988), Numerical Modeling of the Thermal and Hydrological Environment Around a Nuclear Waste Package Using the Equivalent Continuum Approximation: Horizontal Emplacement, Lawrence Livermore National Laboratory, Livermore, CA, UCID-21444. (NNA.890317.0021)

Nitao, J. J. (1991), *Theory of Matrix and Fracture Flow Regimes in Unsaturated, Fractured Porous Media*, Lawrence Livermore National Laboratory, Livermore, CA, UCRL-JC-104933. (NNA.910523.0117)

Nitao, J. J., and T. A. Buscheck (1989), "On the Infiltration of a Liquid Front in an Unsaturated, Fractured Porous Medium," *Proc. of the ANS Topical Mtg on Nuclear Waste Isolation in an Unsaturated Zone, Focus '89* (Amer. Nuc. Soc., La Grange, IL). (Readily available)

O'Neal, W. C., D. W. Gregg, J. N. Hockman, E. W. Russell, and W. Stein (1984), *Preclosure Analysis of Conceptual Waste Package Designs for a Nuclear Waste Repository in Tuff*, Lawrence Livermore National Laboratory, Livermore, CA, UCRL-53595. (NNA.891026.0013)

Ortiz, T. S., R. L. Williams, F. B. Nimick, B. C. Whittet, and D. L. South (1985), *A Three-Dimensional Model of Reference Thermal/Mechanical and Hydrologic Stratigraphy at Yucca Mountain, Southern Nevada*, Sandia National Laboratories, Albuquerque, NM, SAND84-1076. (NNA.890315.0013)

Price, R. H. (1986), *Effects of Sample Size on the Mechanical Behavior of Topopah Spring Tuff*, Sandia National Laboratories, Albuquerque, NM, SAND85-0709. (NNA.891106.0125)

Price, R. H., J. R. Connolly, and K. Keil (1987), *Petrologic and Mechanical Properties of Outcrop Samples of the Welded, Devitrified Topopah Spring Member of the Paintbrush Tuff*, Sandia National Laboratories, Albuquerque, NM, SAND86-1131. (NNA.870601.0013)

Price, R. H., F. B. Nimick, J. R. Connolly, K. Keil, B. M. Schwartz, and S. J. Spense (1985), Preliminary Characterization of the Petrologic, Bulk, and Mechanical Properties of a Lithophysal Zone Within the Topopah Spring Member of the Paintbrush Tuff, Sandia National Laboratories, Albuquerque, NM, SAND84-0860. (NNA.870406.0156)

Ramirez, A., T. Buscheck, R. Carlson, W. Daily, K. Lee, W. Lin, N-H. Mao, T-S. Ueng, H. Wang, and D. Watwood (1991), *Prototype Engineered Barrier System Field Tests (PEBSFT), Final Report*, Lawrence Livermore National Laboratory, Livermore, CA, UCRL-ID-106159. (NNA910711.0047)

Reed, D. T., and R. A. Van Konynenburg (1991), "Corrosion of Copper-Based Materials in Irradiated Moist Air Systems," *Mat. Res. Soc. Symp. Proc.: Scientific Basis for Nucl. Waste Mgmt. XIV*, T. Abrajano, Jr. and L. H. Johnson, Eds. (Mat. Res. Soc., Pittsburg, PA), vol. 212, pp. 317–325. (NNA.911212.0240)

Reed, D. T., V. Swayambunathan, B. S. Tani, and R. A. Van Konynenburg (1990), "Corrosion Product Identification and Relative Rates of Corrosion of Candidate Metals in an Irradiated Air-Steam Environment," *Mat. Res. Soc. Symp. Proc.: Scientific Basis for Nucl. Waste Mgmt. XIII* (Mat. Res. Soc., Pittsburg, PA), p. 517. (NNA.900712.0143)

Scott, R. B., and M. Catellanos (1984), Stratigraphic and Structural Relations of Volcanic Rocks in Drill Holes USW GU-3 and USW G-3, Yucca Mountain, Nye County, Nevada, U.S. Geological Survey, Denver, CO, OFR-84-491. (NNA.870519.0095)

Stock, J. M., J. H. Healy, and S. H. Hickman (1984), *Report on Televiewer Log and Stress Measurements in Core Hole USW G-2, Nevada Test Site*, U.S. Geological Survey, Denver, CO, OFR-84-172. (NNA.870406.0157)

Stock, J. M., J. H. Healy, S. H. Hickman, and M. D. Zoback (1985), "Hydraulic Fracturing Stress Measurements at Yucca Mountain, Nevada, and Relationship to Regional Stress Field," *J. Geophys. Res.* 90(B10), 8691–8706. (Readily available)

Subramanian, C. V., J. L. King, D. M. Perkias, R. W. Modd, A. M. Richardson, J. C. Calovini, E. VanEeckhout, and D. D. Emerson (1990), *Exploratory Shaft Seismic Design Basis Working Group Report*, Sandia National Laboratories, Albuquerque, NM, SAND88-1203. (NNA.911025.0064)

Thorstenson, D. C., E. P. Weeks, H. Haas, and J. C. Woodward (1989), "Physical and Chemical Characteristics of Topographically Affected Airflow in an Open Borehole at Yucca Mountain, Nevada," *Proc. ANS Topical Mtg. on Nuclear Waste Isolation in an Unsaturated Zone, Focus '89*, (Am. Nuc. Soc., La Grange, IL). (NNA.900723.0196)

Van Konynenburg, R. A. (1986), *Radiation Doses in Granite Around Emplacement Holes in the Spent Fuel Test—Climax (Final Report)*, Lawrence Livermore National Laboratory, Livermore, CA, UCRL-53580. (NNA.870903.0040)

Vortman, L. J. (1980), Prediction of Ground Motion from Underground Nuclear Weapons Tests As It Relates to Siting a Nuclear Waste Storage Facility at NTS and Compatibility With the Weapons Test Program, Sandia National Laboratories, Albuquerque, NM, SAND80-1020/1. (NNA.870406.0160)

Wilder, D. G. (1990), "Engineered Barrier Systems and Canister Orientation Studies for the Yucca Mountain Project, Nevada," *Proc. Int. Symp. on Unique Underground Structures* (Colorado School of Mines Press, Colorado). (NNA.910711.0041)